Fully strange tetraquark $ss\bar{s}\bar{s}$ spectrum and possible experimental evidence

Feng-Xiao Liu [1,2] Ming-Sheng Liu,[1,2] Xian-Hui Zhong,[1,2,*] and Qiang Zhao[3,4,2,†]

[1]*Department of Physics, Hunan Normal University, and Key Laboratory of Low-Dimensional Quantum Structures and Quantum Control of Ministry of Education, Changsha 410081, China*
[2]*Synergetic Innovation Center for Quantum Effects and Applications (SICQEA), Hunan Normal University, Changsha 410081, China*
[3]*Institute of High Energy Physics, Chinese Academy of Sciences, Beijing 100049, China*
[4]*University of Chinese Academy of Sciences, Beijing 100049, China*

In this work, we construct 36 tetraquark configurations for the 1*S*-, 1*P*-, and 2*S*-wave states, and make a prediction of the mass spectrum for the tetraquark $ss\bar{s}\bar{s}$ system in the framework of a nonrelativistic potential quark model without the diquark-antidiquark approximation. The model parameters are well determined by our previous study of the strangeonium spectrum. We find that the resonances $f_0(2200)$ and $f_2(2340)$ may favor the assignments of ground states $T_{(ss\bar{s}\bar{s})0^{++}}(2218)$ and $T_{(ss\bar{s}\bar{s})2^{++}}(2378)$, respectively, and the newly observed $X(2500)$ at BESIII may be a candidate of the lowest mass 1*P*-wave 0^{-+} state $T_{(ss\bar{s}\bar{s})0^{-+}}(2481)$. Signals for the other 0^{++} ground state $T_{(ss\bar{s}\bar{s})0^{++}}(2440)$ may also have been observed in the $\phi\phi$ invariant mass spectrum in $J/\psi \to \gamma\phi\phi$ at BESIII. The masses of the $J^{PC} = 1^{--}$ $T_{ss\bar{s}\bar{s}}$ states are predicted to be in the range of $\sim$2.44–2.99 GeV, which indicates that the $\phi(2170)$ resonance may not be a good candidate of the $T_{ss\bar{s}\bar{s}}$ state. This study may provide a useful guidance for searching for the $T_{ss\bar{s}\bar{s}}$ states in experiments.

I. INTRODUCTION

From the Review of Particle Physics (RPP) of Particle Data Group [1], above the mass range of 2.0 GeV one can see that there are several unflavored $q\bar{q}$ isoscaler states, such as $f_0(2200)$, $f_2(2150)$, $f_2(2300)$, $f_2(2340)$, etc., dominantly decaying into $\phi\phi$, $\eta\eta$, and/or $K\bar{K}$ final states. The decay modes indicate that these states might be good candidates for conventional $s\bar{s}$ meson resonances. Recently, we carried out a systematical study of the mass spectrum and strong decay properties of the $s\bar{s}$ system in Ref. [2]. It shows that these states cannot be easily accommodated by the conventional $s\bar{s}$ meson spectrum. While they may be candidates for tetraquark $ss\bar{s}\bar{s}$ ($T_{ss\bar{s}\bar{s}}$) states, it is easy to understand that they can fall apart into $\phi\phi$ and $\eta\eta$ final states through quark rearrangements, or easily decay into $K\bar{K}$ final states through a pair of $s\bar{s}$ annihilations and then a pair of light quark creations. The mass analysis with the relativistic quark model in Ref. [3] supports the $f_0(2200)$

and $f_2(2340)$ to be assigned as the $T_{ss\bar{s}\bar{s}}$ ground states with 0^{++} and 2^{++}, respectively. However, a relativized quark model calculation [4] only favors $f_2(2300)$ to be a $T_{ss\bar{s}\bar{s}}$ state.

Some other candidates of the $T_{ss\bar{s}\bar{s}}$ states from experiment are also suggested in the literature. For example, the vector meson resonance $\phi(2170)$ listed in RPP [1] is suggested to be a 1^{--} $T_{ss\bar{s}\bar{s}}$ state based on the mass analysis of QCD sum rules [5–9] and flux-tube model [10]. The newly observed $X(2239)$ resonance in the $e^+e^- \to K^+K^-$ process at BESIII [11] is suggested to be a candidate of the lowest 1^{--} $T_{ss\bar{s}\bar{s}}$ state in a relativized quark model [4]. Moreover, the newly observed resonances $X(2500)$ observed in $J/\psi \to \gamma\phi\phi$ [12] and $X(2060)$ observed in $J/\psi \to \phi\eta\eta'$ [13] at BESIII are suggested to be 0^{-+} and 1^{+-} $T_{ss\bar{s}\bar{s}}$ states, respectively, according to the QCD sum rule studies [14,15]. The assignment of $X(2500)$ is consistent with that in Ref. [4].

With the recent experimental progresses, more quantitative studies on the $T_{ss\bar{s}\bar{s}}$ states can be carried out and their evidences can also be searched for in experiments. Very recently, the LHCb Collaboration reported their results on the observations of tetraquark $cc\bar{c}\bar{c}$ ($T_{cc\bar{c}\bar{c}}$) states [16]. A broad structure above the $J/\psi J/\psi$ threshold ranging from 6.2 to 6.8 GeV and a narrower structure $T_{cc\bar{c}\bar{c}}(6900)$ are observed with more than 5σ of significance level. There are also some vague structure around 7.2 GeV to be confirmed.

*zhongxh@hunnu.edu.cn
†zhaoq@ihep.ac.cn

These observations could be evidences for genuine $T_{cc\bar{c}\bar{c}}$ states [17–21].

The observations of the $T_{cc\bar{c}\bar{c}}$ states above the $J/\psi J/\psi$ threshold at LHCb may provide an important clue for the underlying dynamics for the $cc\bar{c}\bar{c}$ system. In particular, the narrowness of $T_{cc\bar{c}\bar{c}}(6900)$ suggests that there should be more profound mechanism that "slows down" the fall-apart decays of such a tetraquark system. Although this may be related to the properties of the static potential of heavy quark systems, more direct evidences are still needed to disentangle the dynamical features between the heavy and light flavor systems. As an analogy of the $T_{cc\bar{c}\bar{c}}$ system, there might exist stable $T_{ss\bar{s}\bar{s}}$ states above the $\phi\phi$ threshold and can likely be observed in the di-ϕ mass spectrum. On the other hand, flavor mixings could be important for the light flavor systems and pure $ss\bar{s}\bar{s}$ states may not exist. To answer such questions, systematic calculations of the $ss\bar{s}\bar{s}$ system should be carried out. The BESIII experiments can provide a large data sample for the search of the $T_{ss\bar{s}\bar{s}}$ states in J/ψ and $\psi(2S)$ decays. In theory, although there have been some predictions of the $T_{ss\bar{s}\bar{s}}$ spectrum within the quark model [3,4,10] and QCD sum rules [17–20], most of the studies focus on some special states in a diquark-antidiquark picture. About the status of the tetraquark states, some recent review works can be referenced [22,23]. In this study, we intend to provide a systematical calculation of the mass spectrum of the $1S$, $1P$, and $2S$-wave $T_{ss\bar{s}\bar{s}}$ states without the diquark-antidiquark approximation in a nonrelativistic potential quark model (NRPQM).

The NRPQM is based on the Hamiltonian proposed by the Cornell model [24], which contains a linear confinement and a one-gluon-exchange potential for quark-quark and quark-antiquark interactions. With the NRPQM, we have successfully described the $s\bar{s}$, $c\bar{c}$, and $b\bar{b}$ meson spectra [2,25,26], and sss, ccc, and bbb baryon spectra [27,28]. Furthermore, we adopted the NRPQM for the study of both $1S$ and $1P$-wave all-heavy tetraquark states with a Gaussian expansion method (GEM) [21,29]. In this work, we continue to extend this method to study the $T_{ss\bar{s}\bar{s}}$ spectrum by constructing the full tetraquark configurations without the diquark-antidiquark approximation. With the parameters determined in our study of the $s\bar{s}$ spectrum [2], we obtain a relatively reliable prediction of the mass spectrum for 36 $T_{ss\bar{s}\bar{s}}$ states, i.e., 4 $1S$-wave ground states, 20 $1P$-wave orbital excitations, and 12 $2S$-wave radial excitations.

The paper is organized as follows: a brief introduction to the tetraquark spectrum is given in Sec. II. In Sec. III, the numerical results and discussions are presented. A short summary is given in Sec. IV.

II. MASS SPECTRUM

A. Hamiltonian

We adopt a NRPQM to calculate the mass spectrum of the $ss\bar{s}\bar{s}$ system. In this model, the Hamiltonian is given by

$$H = \left(\sum_{i=1}^{4} m_i + T_i \right) - T_G + \sum_{i<j} V_{ij}(r_{ij}), \qquad (1)$$

where m_i and T_i stand for the constituent quark mass and kinetic energy of the ith quark, respectively; T_G stands for the center-of-mass (c.m.) kinetic energy of the tetraquark system, $r_{ij} \equiv |\mathbf{r}_i - \mathbf{r}_j|$ is the distance between the ith and jth quark, and $V_{ij}(r_{ij})$ stands for the effective potential between them. In this work, the $V_{ij}(r_{ij})$ adopts a widely used form [24–26,30–36]

$$V_{ij}(r_{ij}) = V_{ij}^{\text{conf}}(r_{ij}) + V_{ij}^{sd}(r_{ij}), \qquad (2)$$

where the confinement potential adopts the standard form of the Cornell potential [24], which includes the spin-independent linear confinement potential $V_{ij}^{\text{Lin}}(r_{ij}) \propto r_{ij}$ and Coulomb-like potential $V_{ij}^{\text{Coul}}(r_{ij}) \propto 1/r_{ij}$,

$$V_{ij}^{\text{conf}}(r_{ij}) = -\frac{3}{16}(\lambda_i \cdot \lambda_j)\left(b_{ij}r_{ij} - \frac{4}{3}\frac{\alpha_{ij}}{r_{ij}} + C_0 \right). \quad (3)$$

The constant C_0 stands for the zero point energy. While the spin-dependent potential $V_{ij}^{sd}(r_{ij})$ is the sum of the spin-spin contact hyperfine potential V_{ij}^{SS}, the spin-orbit potential V_{ij}^{SS}, and the tensor term V_{ij}^{T},

$$V_{ij}^{sd}(r_{ij}) = V_{ij}^{SS} + V_{ij}^{T} + V_{ij}^{LS}, \qquad (4)$$

with

$$V_{ij}^{SS} = -\frac{\alpha_{ij}}{4}(\lambda_i \cdot \lambda_j)\left\{ \frac{\pi}{2} \cdot \frac{\sigma_{ij}^3 e^{-\sigma_{ij}^2 r_{ij}^2}}{\pi^{3/2}} \cdot \frac{16}{3m_i m_j}(\mathbf{S}_i \cdot \mathbf{S}_j) \right\}, \quad (5)$$

$$V_{ij}^{LS} = -\frac{\alpha_{ij}}{16}\frac{\lambda_i \cdot \lambda_j}{r_{ij}^3}\left(\frac{1}{m_i^2} + \frac{1}{m_j^2} + \frac{4}{m_i m_j} \right)\{\mathbf{L}_{ij} \cdot (\mathbf{S}_i + \mathbf{S}_j)\}$$
$$- \frac{\alpha_{ij}}{16}\frac{\lambda_i \cdot \lambda_j}{r_{ij}^3}\left(\frac{1}{m_i^2} - \frac{1}{m_j^2} \right)\{\mathbf{L}_{ij} \cdot (\mathbf{S}_i - \mathbf{S}_j)\}, \quad (6)$$

$$V_{ij}^{T} = -\frac{\alpha_{ij}}{4}(\lambda_i \cdot \lambda_j) \cdot \frac{1}{m_i m_j r_{ij}^3}\left\{ \frac{3(\mathbf{S}_i \cdot \mathbf{r}_{ij})(\mathbf{S}_j \cdot \mathbf{r}_{ij})}{r_{ij}^2} - \mathbf{S}_i \cdot \mathbf{S}_j \right\}. \quad (7)$$

In the above equations, $\mathbf{S}_i$ stands for the spin of the ith quark, and $\mathbf{L}_{ij}$ stands for the relative orbital angular momentum between the ith and jth quark. If the interaction occurs between two quarks or antiquarks, the $\lambda_i \cdot \lambda_j$ operator is defined as $\lambda_i \cdot \lambda_j \equiv \sum_{a=1}^{8} \lambda_i^a \lambda_j^a$, while if the interaction occurs between a quark and an antiquark, the $\lambda_i \cdot \lambda_j$ operator is defined as $\lambda_i \cdot \lambda_j \equiv \sum_{a=1}^{8} -\lambda_i^a \lambda_j^{a*}$, where λ^{a*} is the complex conjugate of the Gell-Mann matrix λ^a. The parameters b_{ij} and α_{ij} denote the strength of the

m_s (GeV)	0.60
α_{ss}	0.77
σ_{ss} (GeV)	0.60
b (GeV^2)	0.135
C_0 (GeV)	-0.519

confinement and strong coupling of the one-gluon-exchange potential, respectively.

The five parameters m_s, α_{ss}, σ_{ss}, b_{ss}, and C_0 have been determined by fitting the mass spectrum of the strangeonium in our previous work [2]. The quark model parameters adopted in this work are collected in Table I.

B. Configurations classified in the quark model

To calculate the spectroscopy of a $qq\bar{q}\bar{q}$ ($q \in \{s, c, b\}$) system, first we construct the configurations in the product space of flavor, color, spin, and spatial parts.

In the color space, there are two color-singlet bases $|6\bar{6}\rangle_c$ and $|\bar{3}3\rangle_c$, and their wave functions are given by

$$|6\bar{6}\rangle_c = \frac{1}{2\sqrt{6}}[(rb + br)(\bar{b}\,\bar{r} + \bar{r}\,\bar{b}) + (gr + rg)(\bar{g}\,\bar{r} + \bar{r}\,\bar{g})$$
$$+ (gb + bg)(\bar{b}\,\bar{g} + \bar{g}\,\bar{b})$$
$$+ 2(rr)(\bar{r}\,\bar{r}) + 2(gg)(\bar{g}\,\bar{g}) + 2(bb)(\bar{b}\,\bar{b})], \quad (8)$$

$$|\bar{3}3\rangle_c = \frac{1}{2\sqrt{3}}[(br - rb)(\bar{b}\,\bar{r} - \bar{r}\,\bar{b}) - (rg - gr)(\bar{g}\,\bar{r} - \bar{r}\,\bar{g})$$
$$+ (bg - gb)(\bar{b}\,\bar{g} - \bar{g}\,\bar{b})]. \quad (9)$$

In the spin space, there are six spin bases, which are denoted by $\chi_S^{S_{12}S_{34}}$. Where S_{12} stands for the spin quantum numbers for the diquark $(q_1 q_2)$ (or antidiquark $(\bar{q}_1\bar{q}_2)$), while S_{34} stands for the spin quantum number for the antidiquark $(\bar{q}_3\bar{q}_4)$ (or diquark $(q_3 q_4)$). S is the total spin quantum number of the tetraquark $qq\bar{q}\bar{q}$ system. The spin wave functions $\chi_{SS_z}^{S_{12}S_{34}}$ with a determined S_z (S_z stands for the third component of the total spin $\mathbf{S}$) can be explicitly expressed as follows:

$$\chi_{00}^{00} = \frac{1}{2}(\uparrow\downarrow\uparrow\downarrow - \uparrow\downarrow\downarrow\uparrow - \downarrow\uparrow\uparrow\downarrow + \downarrow\uparrow\downarrow\uparrow), \quad (10)$$

$$\chi_{00}^{11} = \sqrt{\frac{1}{12}}(2\uparrow\uparrow\downarrow\downarrow - \uparrow\downarrow\uparrow\downarrow - \uparrow\downarrow\downarrow\uparrow$$
$$- \downarrow\uparrow\uparrow\downarrow - \downarrow\uparrow\downarrow\uparrow + 2\downarrow\downarrow\uparrow\uparrow), \quad (11)$$

$$\chi_{11}^{01} = \sqrt{\frac{1}{2}}(\uparrow\downarrow\uparrow\uparrow - \downarrow\uparrow\uparrow\uparrow), \quad (12)$$

$$\chi_{11}^{10} = \sqrt{\frac{1}{2}}(\uparrow\uparrow\uparrow\downarrow - \uparrow\uparrow\downarrow\uparrow), \quad (13)$$

$$\chi_{11}^{11} = \frac{1}{2}(\uparrow\uparrow\uparrow\downarrow + \uparrow\uparrow\downarrow\uparrow - \uparrow\downarrow\uparrow\uparrow - \downarrow\uparrow\uparrow\uparrow), \quad (14)$$

$$\chi_{22}^{11} = \uparrow\uparrow\uparrow\uparrow. \quad (15)$$

In the spatial space, we define the relative Jacobi coordinates with the single-partial coordinates $\mathbf{r}_i$ ($i = 1,$ 2, 3, 4),

$$\boldsymbol{\xi}_1 \equiv \mathbf{r}_1 - \mathbf{r}_2, \quad (16)$$

$$\boldsymbol{\xi}_2 \equiv \mathbf{r}_3 - \mathbf{r}_4, \quad (17)$$

$$\boldsymbol{\xi}_3 \equiv \frac{m_1\mathbf{r}_1 + m_2\mathbf{r}_2}{m_1 + m_2} - \frac{m_3\mathbf{r}_3 + m_4\mathbf{r}_4}{m_3 + m_4}, \quad (18)$$

$$\mathbf{R} \equiv \frac{m_1\mathbf{r}_1 + m_2\mathbf{r}_2 + m_3\mathbf{r}_3 + m_4\mathbf{r}_4}{m_1 + m_2 + m_3 + m_4}. \quad (19)$$

Note that $\boldsymbol{\xi}_1$ and $\boldsymbol{\xi}_2$ stand for the relative Jacobi coordinates between two quarks q_1 and q_2 (or antiquarks $\bar{q}_1$ and $\bar{q}_2$), and two antiquarks $\bar{q}_3$ and $\bar{q}_4$ (or quarks q_3 and q_4), respectively. While $\boldsymbol{\xi}_3$ stands for the relative Jacobi coordinate between diquark qq and antidiquark $\bar{q}\,\bar{q}$. Using the above Jacobi coordinates, it is easy to obtain basis functions that have well-defined symmetry under permutations of the pairs (12) and (34) [37].

In the Jacobi coordinate system, the spatial wave function $\Psi_{NLM}(\boldsymbol{\xi}_1, \boldsymbol{\xi}_2, \boldsymbol{\xi}_3, \mathbf{R})$ for a $qq\bar{q}\bar{q}$ system with principal quantum number N and orbital angular momentum quantum numbers LM may be expressed as the linear combination of $\Phi(\mathbf{R})\psi_{\alpha_1}(\boldsymbol{\xi}_1)\psi_{\alpha_2}(\boldsymbol{\xi}_2)\psi_{\alpha_3}(\boldsymbol{\xi}_3)$,

$$\Psi_{NLM}(\boldsymbol{\xi}_1, \boldsymbol{\xi}_2, \boldsymbol{\xi}_3, \mathbf{R})$$
$$= \sum_{\alpha_1, \alpha_2, \alpha_3} C_{\alpha_1, \alpha_2, \alpha_3}[\Phi(\mathbf{R})\psi_{\alpha_1}(\boldsymbol{\xi}_1)\psi_{\alpha_2}(\boldsymbol{\xi}_2)\psi_{\alpha_3}(\boldsymbol{\xi}_3)]_{NLM}, \quad (20)$$

where $C_{\alpha_1, \alpha_2, \alpha_3}$ stands for the combination coefficients, $\Phi(\mathbf{R})$ is the c.m. motion wave function. In the quantum number set $\alpha_i \equiv \{n_{\xi_i}, l_{\xi_i}, m_{\xi_i}\}$, n_{ξ_i} is the principal quantum number, l_{ξ_i} is the angular momentum, and m_{ξ_i} is its third component projection. The wave functions $\psi_{\alpha_i}(\boldsymbol{\xi}_i)$, which account for the relative motions, can be written as

$$\psi_{\alpha_i}(\boldsymbol{\xi}_i) = R_{n_{\xi_i} l_{\xi_i}}(\xi_i) Y_{l_{\xi_i} m_{\xi_i}}(\hat{\boldsymbol{\xi}}_i), \quad (21)$$

where $Y_{l_{\xi_i} m_{\xi_i}}(\hat{\boldsymbol{\xi}}_i)$ is the spherical harmonic function, and $R_{n_{\xi_i} l_{\xi_i}}(\xi_i)$ is the radial part. It is seen that for an excited state, there are three spatial excitation modes corresponding to three independent internal wave functions $\psi_{\alpha_i}(\boldsymbol{\xi}_i)$ ($i = 1,$ 2, 3), which are denoted as ξ_1, ξ_2, and ξ_3, respectively, in the present work. One point should be emphasized that considering the fact that the $ss\bar{s}\bar{s}$ system is composed of equal mass constituent quarks and antiquarks, we adopt a

TABLE II.   Configurations for the tetraquark $qq\bar{q}\bar{q}$ system up to the 2S-wave states.

$J^{P(C)}$	Configuration	Wave function	
$J^{PC}=0^{++}$	$1^1S_{0^{++}(6\bar6)_c}$	$\psi_{000}^{1S}\chi_{00}^{00}$	$|6\bar6\rangle^c$
$J^{PC}=0^{++}$	$1^1S_{0^{++}(\bar33)_c}$	$\psi_{000}^{1S}\chi_{00}^{11}$	$|\bar33\rangle^c$
$J^{PC}=1^{+-}$	$1^3S_{1^{+-}(\bar33)_c}$	$\psi_{000}^{1S}\chi_{11}^{11}$	$|\bar33\rangle^c$
$J^{PC}=2^{++}$	$1^5S_{2^{++}(\bar33)_c}$	$\psi_{000}^{1S}\chi_{22}^{11}$	$|\bar33\rangle^c$
$J^{PC}=0^{--}$	$1^3P_{0^{--}(6\bar6)_c(\xi_1,\xi_2)}$	$\sqrt{\frac{1}{6}}(\psi_{011}^{\xi_1}\chi_{1-1}^{10}-\psi_{010}^{\xi_1}\chi_{10}^{10}+\psi_{01-1}^{\xi_1}\chi_{11}^{10}-\psi_{011}^{\xi_2}\chi_{1-1}^{01}+\psi_{010}^{\xi_2}\chi_{10}^{01}-\psi_{01-1}^{\xi_2}\chi_{11}^{01})$	$|6\bar6\rangle^c$
$J^{PC}=0^{--}$	$1^3P_{0^{--}(\bar33)_c(\xi_1,\xi_2)}$	$\sqrt{\frac{1}{6}}(\psi_{011}^{\xi_1}\chi_{1-1}^{01}-\psi_{010}^{\xi_1}\chi_{10}^{01}+\psi_{01-1}^{\xi_1}\chi_{11}^{01}-\psi_{011}^{\xi_2}\chi_{1-1}^{10}+\psi_{010}^{\xi_2}\chi_{10}^{10}-\psi_{01-1}^{\xi_2}\chi_{11}^{10})$	$|\bar33\rangle^c$
$J^{PC}=0^{-+}$	$1^3P_{0^{-+}(6\bar6)_c(\xi_1,\xi_2)}$	$\sqrt{\frac{1}{6}}(\psi_{011}^{\xi_1}\chi_{1-1}^{10}-\psi_{010}^{\xi_1}\chi_{10}^{10}+\psi_{01-1}^{\xi_1}\chi_{11}^{10}+\psi_{011}^{\xi_2}\chi_{1-1}^{01}-\psi_{010}^{\xi_2}\chi_{10}^{01}+\psi_{01-1}^{\xi_2}\chi_{11}^{01})$	$|6\bar6\rangle^c$
$J^{PC}=0^{-+}$	$1^3P_{0^{-+}(\bar33)_c(\xi_1,\xi_2)}$	$\sqrt{\frac{1}{6}}(\psi_{011}^{\xi_1}\chi_{1-1}^{01}-\psi_{010}^{\xi_1}\chi_{10}^{01}+\psi_{01-1}^{\xi_1}\chi_{11}^{01}+\psi_{011}^{\xi_2}\chi_{1-1}^{10}-\psi_{010}^{\xi_2}\chi_{10}^{10}+\psi_{01-1}^{\xi_2}\chi_{11}^{10})$	$|\bar33\rangle^c$
$J^{PC}=0^{-+}$	$1^3P_{0^{-+}(\bar33)_c(\xi_3)}$	$\sqrt{\frac{1}{3}}(\psi_{011}^{\xi_3}\chi_{1-1}^{11}-\psi_{010}^{\xi_3}\chi_{10}^{11}+\psi_{01-1}^{\xi_3}\chi_{11}^{11})$	$|\bar33\rangle^c$
$J^{PC}=1^{--}$	$1^3P_{1^{--}(6\bar6)_c(\xi_1,\xi_2)}$	$\frac{1}{2}(\psi_{011}^{\xi_1}\chi_{10}^{10}-\psi_{010}^{\xi_1}\chi_{11}^{10}-\psi_{011}^{\xi_2}\chi_{10}^{01}+\psi_{010}^{\xi_2}\chi_{11}^{01})$	$|6\bar6\rangle^c$
$J^{PC}=1^{--}$	$1^3P_{1^{--}(\bar33)_c(\xi_1,\xi_2)}$	$\frac{1}{2}(\psi_{011}^{\xi_1}\chi_{10}^{01}-\psi_{010}^{\xi_1}\chi_{11}^{01}-\psi_{011}^{\xi_2}\chi_{10}^{10}+\psi_{010}^{\xi_2}\chi_{11}^{10})$	$|\bar33\rangle^c$
$J^{PC}=1^{--}$	$1^5P_{1^{--}(\bar33)_c(\xi_3)}$	$\sqrt{\frac{1}{10}}\psi_{011}^{\xi_3}\chi_{20}^{11}-\sqrt{\frac{3}{10}}\psi_{010}^{\xi_3}\chi_{21}^{11}+\sqrt{\frac{3}{5}}\psi_{01-1}^{\xi_3}\chi_{22}^{11}$	$|\bar33\rangle^c$
$J^{PC}=1^{--}$	$1^1P_{1^{--}(\bar33)_c(\xi_3)}$	$\psi_{011}^{\xi_3}\chi_{00}^{11}$	$|\bar33\rangle^c$
$J^{PC}=1^{--}$	$1^1P_{1^{--}(6\bar6)_c(\xi_3)}$	$\psi_{011}^{\xi_3}\chi_{00}^{00}$	$|6\bar6\rangle^c$
$J^{PC}=1^{-+}$	$1^3P_{1^{-+}(6\bar6)_c(\xi_1,\xi_2)}$	$\frac{1}{2}(\psi_{011}^{\xi_1}\chi_{10}^{10}-\psi_{010}^{\xi_1}\chi_{11}^{10}+\psi_{011}^{\xi_2}\chi_{10}^{01}-\psi_{010}^{\xi_2}\chi_{11}^{01})$	$|6\bar6\rangle^c$
$J^{PC}=1^{-+}$	$1^3P_{1^{-+}(\bar33)_c(\xi_1,\xi_2)}$	$\frac{1}{2}(\psi_{011}^{\xi_1}\chi_{10}^{01}-\psi_{010}^{\xi_1}\chi_{11}^{01}+\psi_{011}^{\xi_2}\chi_{10}^{10}-\psi_{010}^{\xi_2}\chi_{11}^{10})$	$|\bar33\rangle^c$
$J^{PC}=1^{-+}$	$1^3P_{1^{-+}(\bar33)_c(\xi_3)}$	$\sqrt{\frac{1}{2}}(\psi_{011}^{\xi_3}\chi_{10}^{11}-\psi_{010}^{\xi_3}\chi_{11}^{11})$	$|\bar33\rangle^c$
$J^{PC}=2^{--}$	$1^3P_{2^{--}(6\bar6)_c(\xi_1,\xi_2)}$	$\sqrt{\frac{1}{2}}(\psi_{011}^{\xi_1}\chi_{11}^{10}-\psi_{011}^{\xi_2}\chi_{11}^{01})$	$|6\bar6\rangle^c$
$J^{PC}=2^{--}$	$1^3P_{2^{--}(\bar33)_c(\xi_1,\xi_2)}$	$\sqrt{\frac{1}{2}}(\psi_{011}^{\xi_1}\chi_{11}^{01}-\psi_{011}^{\xi_2}\chi_{11}^{10})$	$|\bar33\rangle^c$
$J^{PC}=2^{--}$	$1^5P_{2^{--}(\bar33)_c(\xi_3)}$	$\sqrt{\frac{1}{3}}\psi_{011}^{\xi_3}\chi_{21}^{11}-\sqrt{\frac{2}{3}}\psi_{010}^{\xi_3}\chi_{22}^{11}$	$|\bar33\rangle^c$
$J^{PC}=2^{-+}$	$1^3P_{2^{-+}(6\bar6)_c(\xi_1,\xi_2)}$	$\sqrt{\frac{1}{2}}(\psi_{011}^{\xi_1}\chi_{11}^{10}+\psi_{011}^{\xi_2}\chi_{11}^{01})$	$|6\bar6\rangle^c$
$J^{PC}=2^{-+}$	$1^3P_{2^{-+}(\bar33)_c(\xi_1,\xi_2)}$	$\sqrt{\frac{1}{2}}(\psi_{011}^{\xi_1}\chi_{11}^{01}+\psi_{011}^{\xi_2}\chi_{11}^{10})$	$|\bar33\rangle^c$
$J^{PC}=2^{-+}$	$1^3P_{2^{-+}(\bar33)_c(\xi_3)}$	$\psi_{011}^{\xi_3}\chi_{11}^{11}$	$|\bar33\rangle^c$
$J^{PC}=3^{--}$	$1^5P_{3^{--}(\bar33)_c(\xi_3)}$	$\psi_{011}^{\xi_3}\chi_{22}^{11}$	$|\bar33\rangle^c$
$J^{PC}=0^{+-}$	$2^1S_{0^{+-}(6\bar6)_c(\xi_1,\xi_2)}$	$\sqrt{\frac{1}{2}}(\psi_{100}^{\xi_1}\chi_{00}^{00}-\psi_{100}^{\xi_2}\chi_{00}^{00})$	$|6\bar6\rangle^c$
$J^{PC}=0^{+-}$	$2^1S_{0^{+-}(\bar33)_c(\xi_1,\xi_2)}$	$\sqrt{\frac{1}{2}}(\psi_{100}^{\xi_1}\chi_{00}^{11}-\psi_{100}^{\xi_2}\chi_{00}^{11})$	$|\bar33\rangle^c$
$J^{PC}=0^{++}$	$2^1S_{0^{++}(6\bar6)_c(\xi_1,\xi_2)}$	$\sqrt{\frac{1}{2}}(\psi_{100}^{\xi_1}\chi_{00}^{00}+\psi_{100}^{\xi_2}\chi_{00}^{00})$	$|6\bar6\rangle^c$
$J^{PC}=0^{++}$	$2^1S_{0^{++}(\bar33)_c(\xi_1,\xi_2)}$	$\sqrt{\frac{1}{2}}(\psi_{100}^{\xi_1}\chi_{00}^{11}+\psi_{100}^{\xi_2}\chi_{00}^{11})$	$|\bar33\rangle^c$
$J^{PC}=0^{++}$	$2^1S_{0^{++}(6\bar6)_c(\xi_3)}$	$\psi_{100}^{\xi_3}\chi_{00}^{00}$	$|6\bar6\rangle^c$
$J^{PC}=0^{++}$	$2^1S_{0^{++}(\bar33)_c(\xi_3)}$	$\psi_{100}^{\xi_3}\chi_{00}^{11}$	$|\bar33\rangle^c$
$J^{PC}=1^{+-}$	$2^3S_{1^{+-}(\bar33)_c(\xi_1,\xi_2)}$	$\sqrt{\frac{1}{2}}(\psi_{100}^{\xi_1}\chi_{11}^{11}-\psi_{100}^{\xi_2}\chi_{11}^{11})$	$|\bar33\rangle^c$
$J^{PC}=1^{+-}$	$2^3S_{1^{+-}(\bar33)_c(\xi_3)}$	$\psi_{100}^{\xi_3}\chi_{11}^{11}$	$|\bar33\rangle^c$
$J^{PC}=1^{++}$	$2^3S_{1^{++}(\bar33)_c(\xi_1,\xi_2)}$	$\sqrt{\frac{1}{2}}(\psi_{100}^{\xi_1}\chi_{11}^{11}+\psi_{100}^{\xi_2}\chi_{11}^{11})$	$|\bar33\rangle^c$
$J^{PC}=2^{+-}$	$2^5S_{2^{+-}(\bar33)_c(\xi_1,\xi_2)}$	$\sqrt{\frac{1}{2}}(\psi_{100}^{\xi_1}\chi_{22}^{11}-\psi_{100}^{\xi_2}\chi_{22}^{11})$	$|\bar33\rangle^c$
$J^{PC}=2^{++}$	$2^5S_{2^{++}(\bar33)_c(\xi_1,\xi_2)}$	$\sqrt{\frac{1}{2}}(\psi_{100}^{\xi_1}\chi_{22}^{11}+\psi_{100}^{\xi_2}\chi_{22}^{11})$	$|\bar33\rangle^c$
$J^{PC}=2^{++}$	$2^5S_{2^{++}(\bar33)_c(\xi_3)}$	$\psi_{100}^{\xi_3}\chi_{22}^{11}$	$|\bar33\rangle^c$

single set of Jacobi coordinates in this study as an approximation. In fact, the four-body wave function describing a scalar $ss\bar{s}\bar{s}$ state contains a small contribution of internal angular momentum. This contribution is neglected in our calculations. To precisely treat an N-body system, one can involve several different sets of Jacobi coordinates as those done in Refs. [38–43], or adopt a single set of Jacobi coordinates $X = (\xi_i, \xi_2, \ldots, \xi_{N-1})$ with nondiagonal Gaussians e^{-XAX^T} as those done in Refs. [44–47], where A is a symmetric matrix.

Taking into account the Pauli principle and color confinement for the four-quark system $qq\bar{q}\bar{q}$, we have four configurations for 1S-wave ground states, 20 configurations for the 1P-wave orbital excitations, and 12 configurations for the 2S-wave radial excitations. The spin-parity quantum numbers, notations, and wave functions for these configurations are presented in Table II. With the wave functions for all the configurations, the mass matrix elements of the Hamiltonian can be worked out.

To work out the matrix elements in the coordinate space, we expand the radial part $R_{n_{\xi_i} l_{\xi_i}}(\xi_i)$ with a series of harmonic oscillator functions [21,27],

$$R_{n_{\xi_i} l_{\xi_i}}(\xi_i) = \sum_{\ell=1}^{n} \mathcal{C}_{\xi_i\ell} \phi_{n_{\xi_i} l_{\xi_i}}(\omega_{\xi_i\ell}, \xi_i), \qquad (22)$$

with

$$\phi_{n_{\xi_i} l_{\xi_i}}(\omega_{\xi_i\ell}, \xi_i)$$

$$= (\mu_{\xi_i}\omega_{\xi_i\ell})^{\frac{3}{4}} \left[\frac{2^{l_{\xi_i}+2-n_\xi}(2l_{\xi_i} + 2n_{\xi_i} + 1)!!}{\sqrt{\pi}n_{\xi_i}![(2l_{\xi_i} + 1)!!]^2}\right]^{\frac{1}{2}} (\sqrt{\mu_{\xi_i}\omega_{\xi_i\ell}}\xi_i)^{l_{\xi_i}}$$

$$\times e^{-\frac{1}{2}\mu_{\xi_i}\omega_{\xi_i\ell}\xi_i^2} F\left(-n_{\xi_i}, l_{\xi_i} + \frac{3}{2}, \mu_{\xi_i}\omega_{\xi_i\ell}\xi_i^2\right), \qquad (23)$$

where $F(-n_{\xi_i}, l_{\xi_i} + \frac{3}{2}, \mu_{\xi_i}\omega_{\xi_i\ell}\xi_i^2)$ is the confluent hypergeometric function. It should be pointed out that if there are no radial excitations, the expansion method with harmonic oscillator wave functions (HOEM) is just the same as the Gaussian expansion method adopted in the literature [38,39].

For an $ss\bar{s}\bar{s}$ system, if we ensure that the spatial wave function with Jacobi coordinates can transform into the single particle coordinate system, the harmonic oscillator frequencies $\omega_{\xi_i\ell}$ ($i = 1, 2, 3$) can be related to the harmonic oscillator stiffness factor K_ℓ with $\omega_{\xi_1\ell} = \sqrt{2K_\ell/\mu_{\xi_1}}$, $\omega_{\xi_2\ell} = \sqrt{2K_\ell/\mu_{\xi_2}}$, and $\omega_{\xi_3\ell} = \sqrt{4K_\ell/\mu_{\xi_3}}$. Considering the reduced masses $\mu_{\xi_1} = \mu_{\xi_2} = m_s/2$, $\mu_{\xi_3} = m_s$ for $T_{(ss\bar{s}\bar{s})}$, one has $\omega_{\xi_1\ell} = \omega_{\xi_2\ell} = \omega_{\xi_3\ell} = \sqrt{4K_\ell/m_s}$. It indicates that the harmonic oscillator frequencies $\omega_{\xi_i\ell}$ for $T_{(ss\bar{s}\bar{s})}$ are not independent. According to the relation $\omega_{\xi_1\ell} = \omega_{\xi_2\ell} = \omega_{\xi_3\ell} = \omega_\ell$, the expansion of $\prod_{i=1}^{3} R_{n_{\xi_i} l_{\xi_i}}(\xi_i)$ can be simplified as
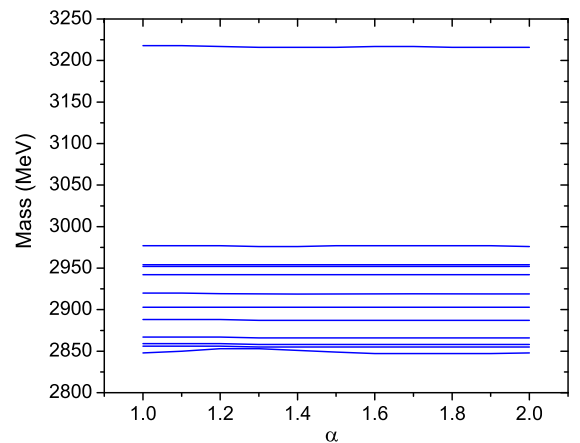
$$\prod_{i=1}^{3} R_{n_{\xi_i} l_{\xi_i}}(\xi_i) = \sum_{\ell}^{n}\sum_{\ell'}^{n}\sum_{\ell''}^{n} \mathcal{C}_{\xi_1\ell}\mathcal{C}_{\xi_2\ell'}\mathcal{C}_{\xi_3\ell''}\phi_{n_{\xi_1} l_{\xi_1}}(\omega_{\xi_1\ell}, \xi_1)\phi_{n_{\xi_2} l_{\xi_2}}(\omega_{\xi_2\ell'}, \xi_2)\phi_{n_{\xi_3} l_{\xi_3}}(\omega_{\xi_3\ell''}, \xi_3)\delta_{\ell\ell'}\delta_{\ell\ell''}$$

$$= \sum_{\ell}^{n} \mathcal{C}_\ell \phi_{n_{\xi_1} l_{\xi_1}}(\omega_\ell, \xi_1)\phi_{n_{\xi_2} l_{\xi_2}}(\omega_\ell, \xi_2)\phi_{n_{\xi_3} l_{\xi_3}}(\omega_\ell, \xi_3). \qquad (24)$$

Then we introduce oscillator length parameters d_ℓ that can be related to the harmonic oscillator frequencies ω_ℓ with $1/d_\ell^2 = m_s\omega_\ell$. Following the method of Refs. [38,39], we let the d_ℓ parameters form a geometric progression

$$d_\ell = d_1 a^{\ell-1} \quad (\ell = 1, \ldots, n), \qquad (25)$$

where n is the number of harmonic oscillator functions and a is the ratio coefficient. There are three parameters $\{d_1, d_n, n\}$ to be determined through the variation method. It is found that with the parameter set $\{0.085$ fm, 3.399 fm, $15\}$ for the $ss\bar{s}\bar{s}$ system, we can obtain stable solutions. The numerical results should be independent of the parameter d_1. To confirm this point, as done in the literature [40–42], we scale the parameter d_1 of the basis functions as $d_1 \rightarrow \alpha d_1$. The mass of a $T_{ss\bar{s}\bar{s}}$ state should be stable at a resonance energy insensitive to the scaling parameter α. As an example, we plot the masses of 12 2S-wave

FIG. 1. Predicted masses of 12 2S-wave $T_{ss\bar{s}\bar{s}}$ configurations as a function of the scaling factor α.

$T_{ss\bar{s}\bar{s}}$ configurations as a function of the scaling factor α in Fig. 1. It is found that the numerical results are nearly independent of the scaling factor α. The stabilization of other states predicted in this work has also been examined by the same method.

With the mass matrix elements ready for each configuration, the mass of the tetraquark configuration and its spacial wave function can be determined by solving a generalized eigenvalue problem. The details can be found in our previous works [27,29]. Finally, the physical states can be obtained by diagonalizing the mass matrix of different configurations with the same J^{PC} numbers.

III. RESULTS AND DISCUSSIONS

Our predictions of the $T_{ss\bar{s}\bar{s}}$ mass spectrum with the HOEM are given in Table III, where the components of different configurations for a physical state can be seen. For example, the two 0^{++} ground states are mixing states between two different configurations $^1S_{0^{++}(6\bar{6})_c}$ and

TABLE III. Predicted mass spectrum for the $ss\bar{s}\bar{s}$ system with the HOEM.

$J^{P(C)}$	Configuration	$\langle H \rangle$ (MeV)	Mass (MeV)	Eigenvector
0^{++}	$1^1S_{0^{++}(6\bar{6})_c}$ $1^1S_{0^{++}(\bar{3}3)_c}$	$\begin{pmatrix} 2365 & -105 \\ -105 & 2293 \end{pmatrix}$	$\begin{pmatrix} 2218 \\ 2440 \end{pmatrix}$	$\begin{pmatrix} (-0.58 & -0.81) \\ (-0.81 & -0.58) \end{pmatrix}$
1^{+-}	$1^3S_{1^{+-}(\bar{3}3)_c}$	(2323)	2323	1
2^{++}	$1^5S_{2^{++}(\bar{3}3)_c}$	(2378)	2378	1
0^{--}	$1^3P_{0^{--}(6\bar{6})_c(\xi_1,\xi_2)}$ $1^3P_{0^{--}(\bar{3}3)_c(\xi_1,\xi_2)}$	$\begin{pmatrix} 2635 & 154 \\ 154 & 2694 \end{pmatrix}$	$\begin{pmatrix} 2507 \\ 2821 \end{pmatrix}$	$\begin{pmatrix} (-0.77 & 0.64) \\ (0.64 & 0.77) \end{pmatrix}$
0^{-+}	$1^3P_{0^{-+}(6\bar{6})_c(\xi_1,\xi_2)}$ $1^3P_{0^{-+}(\bar{3}3)_c(\xi_1,\xi_2)}$ $1^3P_{0^{-+}(\bar{3}3)_c(\xi_3)}$	$\begin{pmatrix} 2616 & -35 & -111 \\ -35 & 2685 & 56 \\ -111 & 56 & 2576 \end{pmatrix}$	$\begin{pmatrix} 2481 \\ 2635 \\ 2761 \end{pmatrix}$	$\begin{pmatrix} (0.61 & -0.11 & 0.78) \\ (-0.56 & -0.76 & 0.34) \\ (0.56 & -0.64 & -0.53) \end{pmatrix}$
1^{--}	$1^3P_{1^{--}(6\bar{6})_c(\xi_1,\xi_2)}$ $1^3P_{1^{--}(\bar{3}3)_c(\xi_1,\xi_2)}$ $1^5P_{1^{--}(\bar{3}3)_c(\xi_3)}$ $1^1P_{1^{--}(\bar{3}3)_c(\xi_3)}$ $1^1P_{1^{--}(6\bar{6})_c(\xi_3)}$	$\begin{pmatrix} 2585 & -154 & -89 & -46 & 90 \\ -154 & 2694 & 42 & 22 & -76 \\ -89 & 42 & 2584 & -8 & 29 \\ -46 & 22 & -8 & 2636 & -51 \\ 90 & -76 & 29 & -51 & 2889 \end{pmatrix}$	$\begin{pmatrix} 2445 \\ 2567 \\ 2627 \\ 2766 \\ 2984 \end{pmatrix}$	$\begin{pmatrix} (-0.80 & -0.38 & -0.43 & -0.14 & 0.11) \\ (0.18 & 0.57 & -0.78 & -0.05 & 0.15) \\ (0.03 & 0.11 & 0.11 & -0.97 & -0.18) \\ (-0.42 & 0.57 & 0.43 & 0.00 & 0.56) \\ (0.38 & -0.43 & -0.07 & -0.19 & 0.79) \end{pmatrix}$
1^{-+}	$1^3P_{1^{-+}(6\bar{6})_c(\xi_1,\xi_2)}$ $1^3P_{1^{-+}(\bar{3}3)_c(\xi_1,\xi_2)}$ $1^3P_{1^{-+}(\bar{3}3)_c(\xi_3)}$	$\begin{pmatrix} 2628 & 95 & 25 \\ 95 & 2712 & 12 \\ 25 & 12 & 2633 \end{pmatrix}$	$\begin{pmatrix} 2564 \\ 2632 \\ 2778 \end{pmatrix}$	$\begin{pmatrix} (0.83 & -0.51 & -0.21) \\ (-0.09 & 0.25 & -0.96) \\ (0.55 & 0.82 & 0.12) \end{pmatrix}$
2^{--}	$1^3P_{2^{--}(6\bar{6})_c(\xi_1,\xi_2)}$ $1^3P_{2^{--}(\bar{3}3)_c(\xi_1,\xi_2)}$ $1^5P_{2^{--}(\bar{3}3)_c(\xi_3)}$	$\begin{pmatrix} 2620 & -217 & -50 \\ -217 & 2725 & 24 \\ -50 & 24 & 2665 \end{pmatrix}$	$\begin{pmatrix} 2446 \\ 2657 \\ 2907 \end{pmatrix}$	$\begin{pmatrix} (0.79 & 0.60 & 0.12) \\ (-0.03 & 0.23 & -0.97) \\ (-0.61 & 0.76 & 0.20) \end{pmatrix}$
2^{-+}	$1^3P_{2^{-+}(6\bar{6})_c(\xi_1,\xi_2)}$ $1^3P_{2^{-+}(\bar{3}3)_c(\xi_1,\xi_2)}$ $1^3P_{2^{-+}(\bar{3}3)_c(\xi_3)}$	$\begin{pmatrix} 2638 & 138 & -33 \\ 138 & 2733 & -16 \\ -33 & -16 & 2673 \end{pmatrix}$	$\begin{pmatrix} 2537 \\ 2669 \\ 2837 \end{pmatrix}$	$\begin{pmatrix} (0.82 & -0.56 & 0.13) \\ (0.00 & 0.23 & 0.97) \\ (-0.58 & -0.79 & 0.19) \end{pmatrix}$
3^{--}	$1^5P_{3^{--}(\bar{3}3)_c(\xi_3)}$	(2719)	2719	1
0^{+-}	$2^1S_{0^{+-}(6\bar{6})_c(\xi_1,\xi_2)}$ $2^1S_{0^{+-}(\bar{3}3)_c(\xi_1,\xi_2)}$	$\begin{pmatrix} 2848 & -27 \\ -27 & 2942 \end{pmatrix}$	$\begin{pmatrix} 2841 \\ 2949 \end{pmatrix}$	$\begin{pmatrix} (-0.97 & -0.26) \\ (-0.26 & 0.97) \end{pmatrix}$
0^{++}	$2^1S_{0^{++}(6\bar{6})_c(\xi_1,\xi_2)}$ $2^1S_{0^{++}(\bar{3}3)_c(\xi_1,\xi_2)}$ $2^1S_{0^{++}(6\bar{6})_c(\xi_3)}$ $2^1S_{0^{++}(\bar{3}3)_c(\xi_3)}$	$\begin{pmatrix} 2859 & -53 & -61 & -18 \\ -53 & 2903 & -20 & -49 \\ -61 & -20 & 3218 & -40 \\ -18 & -49 & -40 & 2856 \end{pmatrix}$	$\begin{pmatrix} 2781 \\ 2876 \\ 2948 \\ 3232 \end{pmatrix}$	$\begin{pmatrix} (-0.61 & -0.52 & -0.16 & -0.57) \\ (0.67 & 0.02 & 0.03 & -0.74) \\ (0.39 & -0.85 & 0.07 & 0.34) \\ (0.15 & 0.02 & -0.98 & 0.09) \end{pmatrix}$
1^{+-}	$2^3S_{1^{+-}(\bar{3}3)_c(\xi_1,\xi_2)}$ $2^3S_{1^{+-}(\bar{3}3)_c(\xi_3)}$	$\begin{pmatrix} 2954 & 0 \\ 0 & 2867 \end{pmatrix}$	$\begin{pmatrix} 2867 \\ 2954 \end{pmatrix}$	$\begin{pmatrix} (0 & 1) \\ (1 & 0) \end{pmatrix}$
1^{++}	$2^3S_{1^{++}(\bar{3}3)_c(\xi_1,\xi_2)}$	(2920)	2920	1
2^{+-}	$2^5S_{2^{+-}(\bar{3}3)_c(\xi_1,\xi_2)}$	(2977)	2977	1
2^{++}	$2^5S_{2^{++}(\bar{3}3)_c(\xi_1,\xi_2)}$ $2^5S_{2^{++}(\bar{3}3)_c(\xi_3)}$	$\begin{pmatrix} 2952 & -28 \\ -28 & 2888 \end{pmatrix}$	$\begin{pmatrix} 2878 \\ 2963 \end{pmatrix}$	$\begin{pmatrix} (-0.35 & -0.94) \\ (-0.94 & 0.35) \end{pmatrix}$

TABLE IV.   The average contributions of each part of the Hamiltonian to the $ss\bar{s}\bar{s}$ configurations with the HOEM. $\langle T \rangle$ stands for the contribution of the kinetic energy term. $\langle V^{\mathrm{Lin}}\rangle$ and $\langle V^{\mathrm{Coul}}\rangle$ stand for the contributions from the linear confinement potential and Coulomb-type potential, respectively. $\langle V^{SS}\rangle$, $\langle V^{T}\rangle$, and $\langle V^{LS}\rangle$ stand for the contributions from the spin-spin interaction term, the tensor potential term, and the spin-orbit interaction term, respectively. The second number in every column is calculated with the GEM.

$J^{P(C)}$	Configuration	Mass	$\langle T \rangle$	$\langle V^{\mathrm{Lin}}\rangle$	$\langle V^{\mathrm{Coul}}\rangle$	$\langle V^{SS}\rangle$	$\langle V^{T}\rangle$	$\langle V^{LS}\rangle$
0^{++}	$1^1S_{0^{++}(6\bar{6})_c}$	2365	807	930	-774	40.07		
	$1^1S_{0^{++}(\bar{3}3)_c}$	2293	884	890	-812	-29.72		
1^{+-}	$1^3S_{1^{+-}(\bar{3}3)_c}$	2323	851	906	-797	0.00		
2^{++}	$1^5S_{2^{++}(\bar{3}3)_c}$	2378	793	937	-767	52.33		
0^{--}	$1^3P_{0^{--}(6\bar{6})_c(\xi_1,\xi_2)}$	2635	827	1077	-659	4.42	34.92	-11.64
	$1^3P_{0^{--}(\bar{3}3)_c(\xi_1,\xi_2)}$	2694	902	1094	-644	-0.95	9.02	-27.06
0^{-+}	$1^3P_{0^{-+}(6\bar{6})_c(\xi_1,\xi_2)}$	2616	862	1056	-675	26.93	-4.20	-12.60
	$1^3P_{0^{-+}(\bar{3}3)_c(\xi_1,\xi_2)}$	2685	921	1083	-651	8.30	-9.39	-28.16
	$1^3P_{0^{-+}(\bar{3}3)_c(\xi_3)}$	2576	976	1015	-703	9.95	-20.88	-62.65
1^{--}	$1^3P_{1^{--}(6\bar{6})_c(\xi_1,\xi_2)}$	2585	895	1037	-688	5.06	-20.11	-6.70
	$1^3P_{1^{--}(\bar{3}3)_c(\xi_1,\xi_2)}$	2694	902	1094	-644	-0.95	-4.51	-13.53
	$1^5P_{1^{--}(\bar{3}3)_c(\xi_3)}$	2584	972	1018	-702	43.08	-14.60	-93.87
	$1^1P_{1^{--}(\bar{3}3)_c(\xi_3)}$	2636	876	1068	-665	-5.24	0	0
	$1^1P_{1^{--}(6\bar{6})_c(\xi_3)}$	2889	847	1210	-564	33.27	0	0
1^{-+}	$1^3P_{1^{-+}(6\bar{6})_c(\xi_1,\xi_2)}$	2628	845	1066	-667	26.33	2.03	-6.08
	$1^3P_{1^{-+}(\bar{3}3)_c(\xi_1,\xi_2)}$	2712	881	1106	-636	8.27	4.33	-13.00
	$1^3P_{1^{-+}(\bar{3}3)_c(\xi_3)}$	2633	883	1064	-668	9.07	8.73	-26.18
2^{--}	$1^3P_{2^{--}(6\bar{6})_c(\xi_1,\xi_2)}$	2620	845	1066	-667	4.59	3.63	6.05
	$1^3P_{2^{--}(\bar{3}3)_c(\xi_1,\xi_2)}$	2725	859	1120	-628	-0.58	0.83	12.40
	$1^5P_{2^{--}(\bar{3}3)_c(\xi_3)}$	2665	845	1087	-652	35.76	11.32	-24.26
2^{-+}	$1^3P_{2^{-+}(6\bar{6})_c(\xi_1,\xi_2)}$	2638	832	1074	-662	25.87	-0.39	5.91
	$1^3P_{2^{-+}(\bar{3}3)_c(\xi_1,\xi_2)}$	2733	854	1123	-626	8.22	-0.82	12.2
	$1^3P_{2^{-+}(\bar{3}3)_c(\xi_3)}$	2673	830	1097	-646	8.52	-1.56	23.43
3^{--}	$1^5P_{3^{--}(\bar{3}3)_c(\xi_3)}$	2719	779	1131	-625	31.92	-2.80	41.96
0^{+-}	$2^1S_{0^{+-}(6\bar{6})_c(\xi_1,\xi_2)}$	2848/2927	703/844	1131/1225	$-363/-529$	14.19/24.74		
	$2^1S_{0^{+-}(\bar{3}3)_c(\xi_1,\xi_2)}$	2942/2931	936/941	1246/1246	$-599/-618$	$-4.09/0.80$		
0^{++}	$2^1S_{0^{++}(6\bar{6})_c(\xi_1,\xi_2)}$	2859/2874	848/863	1177/1206	$-552/-585$	24.92/27.90		
	$2^1S_{0^{++}(\bar{3}3)_c(\xi_1,\xi_2)}$	2903/2918	957/954	1236/1235	$-639/-620$	$-12.68/-12.40$		
	$2^1S_{0^{++}(6\bar{6})_c(\xi_3)}$	3218/3148	898/922	1399/1364	$-469/-517$	27.06/17.52		
	$2^1S_{0^{++}(\bar{3}3)_c(\xi_3)}$	2856/2841	897/899	1186/1197	$-586/-622$	$-3.69/4.74$		
1^{+-}	$2^3S_{1^{+-}(\bar{3}3)_c(\xi_1,\xi_2)}$	2954/2943	921/926	1254/1256	$-591/-614$	7.97/12.47		
	$2^3S_{1^{+-}(\bar{3}3)_c(\xi_3)}$	2867/2851	884/895	1192/1201	$-578/-621$	7.36/14.61		
1^{++}	$c^3S_{1^{++}(\bar{3}3)_c(\xi_1,\xi_2)}$	2920/2934	939/926	1247/1252	$-632/-610$	4.36/3.51		
2^{+-}	$2^5S_{2^{+-}(\bar{3}3)_c(\xi_1,\xi_2)}$	2977/2965	893/905	1270/1271	$-578/-607$	30.15/34.34		
2^{++}	$2^5S_{2^{++}(\bar{3}3)_c(\xi_1,\xi_2)}$	2952/2964	903/898	1267/1272	$-616/-601$	35.64/33.36		
	$2^5S_{2^{++}(\bar{3}3)_c(\xi_3)}$	2888/2871	859/868	1203/1220	$-564/-612$	27.60/33.30		

$^1S_{0^{++}(\bar{3}3)_c}$ due to a strong contribution of the confinement potential to the nondiagonal elements. To see the contributions from each part of the Hamiltonian to the mass of different configurations, we also present our results in Table IV. It is found that both the kinetic energy term $\langle T \rangle$ and the linear confinement potential term $\langle V^{\mathrm{Lin}}\rangle$ contribute a large positive value to the mass, while the Coulomb-type potential $\langle V^{\mathrm{Coul}}\rangle$ has a large cancellation with these two terms. The spin-spin interaction term $\langle V^{SS}\rangle$, the tensor potential term $\langle V^{T}\rangle$, and/or the spin-orbit interaction term $\langle V^{LS}\rangle$ have also sizable contributions to some configurations. Thus, as a reliable
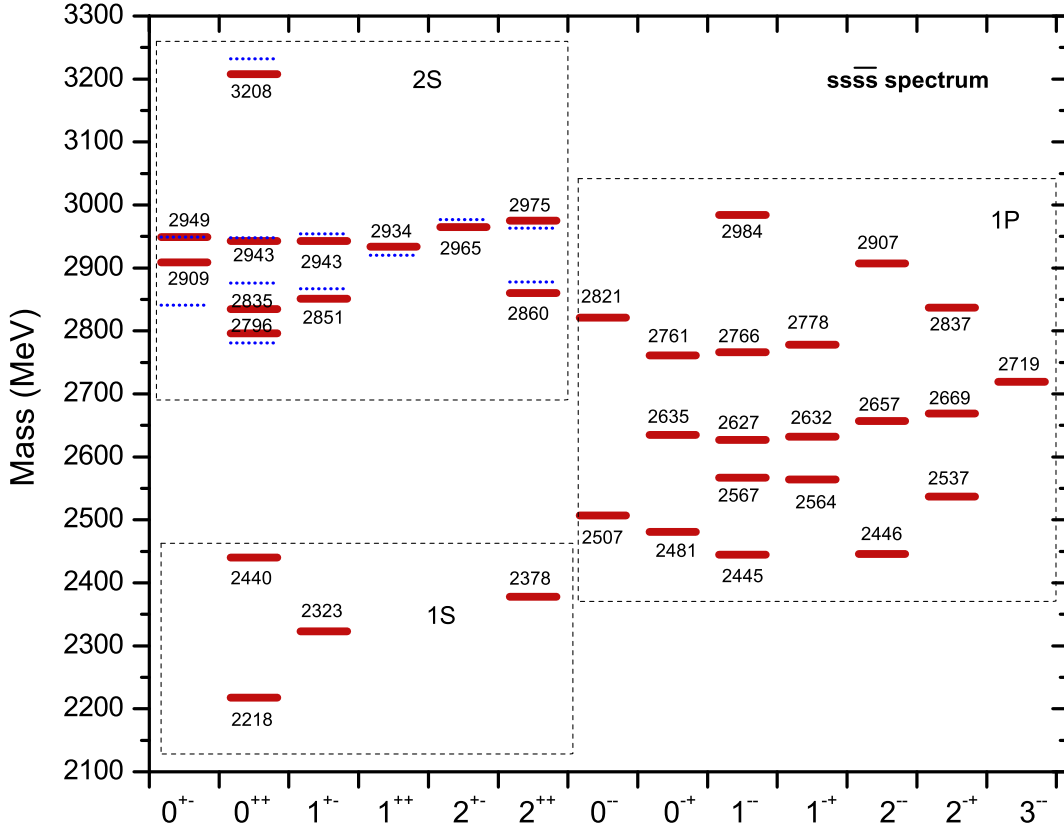
FIG. 2.   Mass spectrum for the $ss\bar{s}\,\bar{s}$ system. The solid and dotted lines stand for the results predicted by the GEM and HOEM, respectively.

calculation, both the spin-independent and spin-dependent potentials should be reasonably included for the $ss\bar{s}\bar{s}$ system. For clarity, our predicted $T_{ss\bar{s}\bar{s}}$ spectrum is plotted in Fig. 2.

A. Discussions of the numerical method

Herein we discuss the differences of numerical results between the HOEM used in present work and the GEM often adopted in the literature. For the $1S$-, $1P$-wave $T_{(ss\bar{s}\bar{s})}$ states, etc., there are no radial excitations. Thus, the GEM is the same as the HOEM. For the first radial excited $2S$-wave $T_{(ss\bar{s}\bar{s})}$ states, the HOEM is different from the GEM because the trail harmonic oscillator wave functions are different from the Gaussian functions.

To see the differences between the two expansion methods, we also give our predictions of the $2S$-wave $T_{(ss\bar{s}\bar{s})}$ states based on the GEM. It should be mentioned that by fully expanding $\prod_{i=1}^{3} R_{n_{\xi_i} l_{\xi_i}}(\xi_i)$ with the GEM, one cannot distinguish the ξ_1 and ξ_2 excited modes which are defined for the $2S$ configurations presented in Table II. Then we cannot numerically work out the masses for the following states of 0^{+-} ($2^1S_{0^{+-}-(6\bar{6})_c(\xi_1,\xi_2)}$ and $2^1S_{0^{+-}-(\bar{3}3)_c(\xi_1,\xi_2)}$), 1^{+-} ($2^3S_{1^{+-}-(\bar{3}3)_c(\xi_1,\xi_2)}$), and 1^{+-} ($2^5S_{2^{+-}-(\bar{3}3)_c(\xi_1,\xi_2)}$) listed in Table II. To overcome this

problem, the spatial wave functions containing the radial excitations are expanded with the Gaussian functions, while the spatial wave functions containing no excitations are adopted the single Gaussian function as an approximation. We have tested the single Gaussian approximation in the calculations of the ground $1S$ $T_{(ss\bar{s}\bar{s})}$ states, the numerical values are reasonably consistent with those calculated with a series of Gaussian functions. The differences of the numerical results between these two methods are about 10 MeV.

Our numerical results for the $2S$-wave $T_{(ss\bar{s}\bar{s})}$ states with the GEM are listed in Tables IV and V. From Table IV, it is found that the numerical values for the 0^{+-} configuration $2^1S_{0^{+-}-(6\bar{6})_c(\xi_1,\xi_2)}$ and 0^{++} configuration $2^1S_{0^{++}-(6\bar{6})_c(\xi_3)}$ calculated with the HOEM are significantly different from those obtained with the GEM. For these two configurations, the predicted mass differences by the HOEM and GEM can reach up to $\sim$70 MeV. However, for the other $2S$-wave $T_{(ss\bar{s}\bar{s})}$ configurations, the numerical values of these two methods are comparable with each other. The differences of the predicted masses between these two methods are about 10–20 MeV. It should be mentioned that the Coulomb-type potential $\langle V^{\text{Coul}} \rangle$ for the $2S$-wave states seems to be sensitive to the numerical methods as shown in Table IV.

TABLE V.   Predicted mass spectrum for the $2S$-wave $ss\bar{s}\bar{s}$ system with the GEM.

J^{PC}	state	matrix	eigenvalues	eigenvectors
0^{+-}	$2^1S_{0^{+-}(6\bar{6})_c(\xi_1,\xi_2)}$ $2^1S_{0^{+-}(\bar{3}3)_c(\xi_1,\xi_2)}$	$\begin{pmatrix} 2927 & -20 \\ -20 & 2931 \end{pmatrix}$	$\begin{pmatrix} 2909 \\ 2949 \end{pmatrix}$	$\begin{pmatrix} (-0.75 & -0.67) \\ (-0.67 & 0.75) \end{pmatrix}$
0^{++}	$2^1S_{0^{++}(6\bar{6})_c(\xi_1,\xi_2)}$ $2^1S_{0^{++}(\bar{3}3)_c(\xi_1,\xi_2)}$ $2^1S_{0^{++}(6\bar{6})_c(\xi_3)}$ $2^1S_{0^{++}(\bar{3}3)_c(\xi_3)}$	$\begin{pmatrix} 2874 & -48 & 134 & -17 \\ -48 & 2918 & -9 & -37 \\ 134 & -9 & 3148 & -31 \\ -17 & -37 & -31 & 2841 \end{pmatrix}$	$\begin{pmatrix} 2796 \\ 2835 \\ 2943 \\ 3208 \end{pmatrix}$	$\begin{pmatrix} (-0.75 & -0.41 & 0.23 & -0.45) \\ (-0.47 & 0.12 & 0.29 & 0.82) \\ (0.25 & -0.90 & -0.15 & 0.33) \\ (-0.38 & 0.08 & -0.92 & 0.09) \end{pmatrix}$
1^{+-}	$2^3S_{1^{+-}(\bar{3}3)_c(\xi_1,\xi_2)}$ $2^3S_{1^{+-}(\bar{3}3)_c(\xi_3)}$	$\begin{pmatrix} 2943 & 0 \\ 0 & 2851 \end{pmatrix}$	$\begin{pmatrix} 2851 \\ 2943 \end{pmatrix}$	$\begin{pmatrix} (0 & 1) \\ (1 & 0) \end{pmatrix}$
1^{++}	$2^3S_{1^{++}(\bar{3}3)_c(\xi_1,\xi_2)}$	(2934)	2934	1
2^{+-}	$2^5S_{2^{+-}(\bar{3}3)_c(\xi_1,\xi_2)}$	(2965)	2965	1
2^{++}	$2^5S_{2^{++}(\bar{3}3)_c(\xi_1,\xi_2)}$ $2^5S_{2^{++}(\bar{3}3)_c(\xi_3)}$	$\begin{pmatrix} 2964 & -33 \\ -33 & 2871 \end{pmatrix}$	$\begin{pmatrix} 2860 \\ 2975 \end{pmatrix}$	$\begin{pmatrix} (-0.30 & -0.95) \\ (-0.95 & 0.30) \end{pmatrix}$

In brief, most of the predictions are consistent with each other between the HOEM and GEM. The uncertainties from the numerical methods do not change our main predictions of the $T_{(ss\bar{s}\bar{s})}$ spectrum. Although some numerical results for the $J^{PC} = 0^{+-}$ and 0^{++} $2S$ states show a significant numerical method dependence (see Fig. 2), the GEM may give a slightly more accurate numerical result based on our tests of the charmonium spectrum. In the following, our discussions of the $2S$ states are based on the GEM calculations.

B. S-wave states

There are four $1S$-wave $T_{ss\bar{s}\bar{s}}$ states with $J^{PC} = 0^{++}$, 1^{+-}, 2^{++} in the quark model. Their masses are predicted to be in the range of 2.21–2.44 GeV. In contrast, the $2S$ wave includes 12 states. Except for the highest mass state $T_{(ss\bar{s}\bar{s})0^{++}}(3208)$, their masses lie in a relative narrow range of 2.78–2.98 GeV. Apart from the conventional quantum numbers, i.e., $J^{PC} = 0^{++}$, 1^{++}, 1^{+-}, 2^{++}, the $2S$-wave can access exotic quantum numbers, i.e., $J^{PC} = 0^{+-}$, 2^{+-}.

1. 0^{++} states

In the $1S$-wave multiplets, the two 0^{++} ground states include $T_{(ss\bar{s}\bar{s})0^{++}}(2218)$ and $T_{(ss\bar{s}\bar{s})0^{++}}(2440)$. Their mass splitting reaches up to about 200 MeV. These two states have a strong mixing between the two color structures $|6\bar{6}\rangle_c$ and $|\bar{3}3\rangle_c$. Their masses are much larger than the mass threshold of $\phi\phi$. Thus, they may easily decay into $\phi\phi$ pair through quark rearrangements. The mass of the lowest 0^{++} $T_{ss\bar{s}\bar{s}}$ in our model is close to the prediction of 2203 MeV in the relativistic diquark-antidiquark model [3]. However, it turns out to be much higher than the predicted value 1716 MeV by the relativized quark model with a diquark-antidiquark approximation [4]. There might be some crucial dynamics missing in the diquark-antidiquark approximation. As a test of the diquark-antidiquark approximation, we adopt the approximation as done in Ref. [4] and

calculate the mass of the 0^{++} $T_{ss\bar{s}\bar{s}}$ state with the same potential model parameters. We obtain a mass of 1758 MeV, which is comparable with the prediction of Ref. [4], but is obviously smaller than the results without the diquark-antidiquark approximation.

In the $2S$-wave sector, there are four 0^{++} states, $T_{(ss\bar{s}\bar{s})0^{++}}(2796)$, $T_{(ss\bar{s}\bar{s})0^{++}}(2835)$, $T_{(ss\bar{s}\bar{s})0^{++}}(2943)$, and $T_{(ss\bar{s}\bar{s})0^{++}}(3208)$, predicted in the NRPQM. A strong mixing between the two color structures $|6\bar{6}\rangle_c$ and $|\bar{3}3\rangle_c$ is also found among these states. In particular, the radial excitation modes (ξ_1,ξ_2) and (ξ_3) strongly mix with each other. The highest state $T_{(ss\bar{s}\bar{s})0^{++}}(3208)$ is nearly a pure configuration of $^1S_{0^{++}(6\bar{6})_c(\xi_3)}$, with the color structure $|6\bar{6}\rangle_c$ and the radial excitation between diquark (ss) and antidiquark $(\bar{s}\bar{s})$. The special color structure of $T_{(ss\bar{s}\bar{s})0^{++}}(3208)$ leads to a rather large mass gap $\Delta \simeq 265$ MeV from the nearby $T_{(ss\bar{s}\bar{s})0^{++}}(2943)$. These $2S$-wave 0^{++} $ss\bar{s}\bar{s}$ states may easily decay into $\phi\phi$, $\phi\phi(1680)$ final states through quark rearrangements. They may also easily decay into $K_s^0 K_s^0$ and $K^+ K^-$ final states through the $s\bar{s}$ annihilation and a pair of nonstrange $q\bar{q}$ creation. One also notices that these states may directly decay into $\Xi\bar{\Xi}$ baryon pair with a light $q\bar{q}$ pair creation.

Some evidences for $T_{(ss\bar{s}\bar{s})0^{++}}(2218)$ and $T_{(ss\bar{s}\bar{s})0^{++}}(2440)$ may have been seen in the previous experiments. Recently, Kozhevnikov carried out a dynamical analysis of the resonance contributions to $J/\psi \to \gamma X \to \gamma\phi\phi$ [48] with the data from BESIII [12]. Two 0^{++} resonances with masses at $\sim$2.2 and $\sim$2.4 GeV were extracted from the data. Evidence for a scalar around 2.2 GeV in the $\phi\phi$ mass spectra in $B_s^0 \to J/\psi\phi\phi$ [49] was also reported by Ref. [50]. Considering the mass and decay mode, these two scalar structures may be good candidates for $T_{(ss\bar{s}\bar{s})0^{++}}(2218)$ and $T_{(ss\bar{s}\bar{s})0^{++}}(2440)$.

It should be mentioned that $f_0(2200)$ is listed in RPP [1] as a well-established state. It has been seen in the $K_s^0 K_s^0$, $K^+ K^-$, and $\eta\eta$, and may be assigned to $T_{(ss\bar{s}\bar{s})0^{++}}(2218)$. Some qualitative features can be expected: (i) the 0^{++} $T_{ss\bar{s}\bar{s}}$

state can decay into $\eta\eta$, $\eta'\eta'$, and $\eta\eta'$ through quark rearrangements via the $s\bar{s}$ component in the η and η' mesons. An approximate branching ratio fraction can be examined: $\mathrm{BR}(\eta\eta):\mathrm{BR}(\eta'\eta'):\mathrm{BR}(\eta\eta') \simeq \sin^4\alpha_P:\cos^4\alpha_P: 2\sin^2\alpha_P\cos^2\alpha_P \simeq 0.24:0.25:0.50$, with $\alpha_P \equiv \arctan\sqrt{2} + \theta_P \simeq 44.7°$ and without including the phase space factors. (ii) The 0^{++} states may also easily decay into $K_s^0 K_s^0$ and K^+K^- final states through annihilating a pair of $s\bar{s}$ and creating a pair of light $q\bar{q}$. (iii) It is interesting to note that no conventional 0^{++} $s\bar{s}$ states are predicted around 2.2 GeV in most literatures [2].

To establish the 0^{++} ground states $T_{(ss\bar{s}\bar{s})0^{++}}(2218)$ and $T_{(ss\bar{s}\bar{s})0^{++}}(2440)$, a combined study of decay channels, such as $\phi\phi$, $K_s^0 K_s^0$, K^+K^-, $\eta\eta$, $\eta'\eta'$, and $\eta\eta'$, should be necessary. The $2S$-wave 0^{++} states can be probed in these meson pair decay channels including higher channels such as $\phi\phi(1680)$, and some baryon pair decay channels such as $\Xi\bar{\Xi}$.

2. 2^{++} states

There is only one 2^{++} state $T_{(ss\bar{s}\bar{s})2^{++}}(2378)$ in the 1S-wave states. This state lies between the two 0^{++} ground states and has a pure $|\bar{3}3\rangle_c$ color structure. $T_{(ss\bar{s}\bar{s})2^{++}}(2378)$ may have large decay rates into the $\phi\phi$, $\eta\eta$, and $\eta'\eta'$ final states through quark rearrangements and/or into $K^{(*)}\bar{K}^{(*)}$ final states through the annihilation of $s\bar{s}$ and creation of a pair of nonstrange $q\bar{q}$. It should be mentioned that with the diquark-antidiquark approximation, the mass of the 2^{++} state is predicted to be 2192 MeV, which is about 200 MeV lower than the four-body calculation results.

The $f_2(2340)$ resonance listed in RPP [1] may be assigned to $T_{(ss\bar{s}\bar{s})2^{++}}(2378)$. Besides the measured mass 2345^{+50}_{-40} MeV, the observed decay modes $\phi\phi$ and $\eta\eta$ are consistent with the expectation of the tetraquark scenario. On the other hand, as a conventional $s\bar{s}$ state, the $f_2(2340)$ cannot be easily accommodated by the quark model expectation [2]. The relativistic quark model calculation of Ref. [3] also supports the $f_2(2340)$ to be assigned as the $T_{ss\bar{s}\bar{s}}$ ground state with 2^{++}. To confirm this assignment, the other main decay modes of $T_{(ss\bar{s}\bar{s})2^{++}}(2378)$ such as $\eta\eta'$, $\eta'\eta'$, $K^{(*)}\bar{K}^{(*)}$ should be investigated in experiment.

For the $2S$-wave sector, there are two 2^{++} $ss\bar{s}\bar{s}$ states $T_{(ss\bar{s}\bar{s})2^{++}}(2860)$ and $T_{(ss\bar{s}\bar{s})2^{++}}(2975)$ predicted in our model, which are dominated by the $^5S_{2^{++}(\bar{3}3)_c(\xi_3)}$ and $^5S_{2^{++}(\bar{3}3)_c(\xi_1,\xi_2)}$ configurations, respectively. Their masses are predicted to be above the thresholds of $\phi\phi$, $\phi\phi(1680)$ and $\Xi(1530)\bar{\Xi}$. Therefore, experimental search for their signals in these decay channels should be helpful for understanding these tensor tetraquarks.

3. 1^{+-} states

In the 1S-wave multiplets, $T_{(ss\bar{s}\bar{s})1^{+-}}(2323)$ is the only state with $C = -1$ and has a pure $|\bar{3}3\rangle_c$ color structure. Its

mass is about 100 MeV larger than the lowest 1S-wave state $T_{(ss\bar{s}\bar{s})0^{++}}(2218)$. Its mass is about 200–300 MeV larger than that predicted by the QCD sum rules [15] and the relativized quark model [4] in the diquark picture. The mass of the 1^{+-} state may be notably underestimated in the diquark picture. As a comparison, we calculate the mass of the 1^{+-} state in the diquark picture using the same potential model parameter set adopted in present work, and obtain a mass of 1936 MeV, which is 300 MeV smaller than the NRQPM prediction 2236 MeV.

$T_{(ss\bar{s}\bar{s})1^{+-}}(2323)$ may easily decay into $\eta\phi$ and $\eta'\phi$ through the quark rearrangements. The decay of $\psi'/J/\psi \to \phi\eta\eta'$ can access this state in $\eta\phi$ and $\eta'\phi$ channels. It should be mentioned that some hints of $T_{(ss\bar{s}\bar{s})1^{+-}}(2323)$ may have been found in the $\eta'\phi$ invariant mass spectrum around 2.3–2.4 GeV by observing the $J/\psi \to \phi\eta\eta'$ reaction at BESIII recently [13].

For the $2S$-wave sector, there are two states, i.e., 1^{+-} $ss\bar{s}\bar{s}$ $T_{(ss\bar{s}\bar{s})1^{+-}}(2851)$ and $T_{(ss\bar{s}\bar{s})1^{+-}}(2943)$ predicted in the quark model. There are no configuration mixings in these two states. $T_{(ss\bar{s}\bar{s})1^{+-}}(2851)$ has a pure $|\bar{3}3\rangle_c$ color structure, and the radial excitation occurs between diquark (ss) and antidiquark $(\bar{s}\bar{s})$ (i.e., the ξ_3 mode). In contrast, although $T_{(ss\bar{s}\bar{s})1^{+-}}(2943)$ has also a pure $|\bar{3}3\rangle_c$ color structure, its radial excitation occurs in the diquark (ss) and antidiquark $(\bar{s}\bar{s})$. Apart from the $\eta\phi$ and $\eta'\phi$ decay channels, it may favor decays into a pseudoscalar plus a radially excited vector [i.e., $\eta\phi(1680)$ and $\eta'\phi(1680)$], or a radially excited pseudoscalar plus a vector [i.e., $\eta(1295)\phi$ and $\eta(1405)\phi$], through the quark rearrangements.

It should be mentioned that in Refs. [9,15] the authors suggest that the new structure $X(2063)$ observed in the $J/\psi \to \phi\eta\eta'$ at BESIII [13] could be a 1^{+-} $T_{ss\bar{s}\bar{s}}$ candidate according to the QCD sum rule calculation. However, the observed mass of $X(2063)$ is too small to be comparable with our quark model predictions.

4. 0^{+-} and 2^{+-} states

In the $2S$-wave multiplets, there are two 0^{+-} states, $T_{(ss\bar{s}\bar{s})0^{+-}}(2909)$ and $T_{(ss\bar{s}\bar{s})0^{+-}}(2949)$, predicted in the NRPQM. There is a strong configuration mixing between $^1S_{0^{+-}(6\bar{6})_c(\xi_1,\xi_2)}$ and $^1S_{0^{+-}(\bar{3}3)_c(\xi_1,\xi_2)}$. There is only one 2^{+-} state $T_{(ss\bar{s}\bar{s})2^{+-}}(2965)$ corresponding to the configuration $^5S_{2^{+-}(\bar{3}3)_c(\xi_1,\xi_2)}$. The 0^{+-} and 2^{+-} are exotic quantum numbers which cannot be accommodated by the conventional $q\bar{q}$ scenario. The P-wave decays into the $\eta h_1(1P)$ and $\eta' h_1(1P)$ channels could be useful for the search for these states in experiments.

C. 1P-wave states

There are twenty 1P-wave $T_{ss\bar{s}\bar{s}}$ states predicted in the NRPQM. Apart from the conventional quantum numbers, i.e., $J^{PC} = 0^{-+}, 1^{--}, 2^{-+}, 2^{--}, 3^{--}$, the P wave can access

exotic quantum numbers, i.e., $J^{PC} = 0^{--}, 1^{-+}$. The masses of the 1P-wave $T_{ss\bar{s}\bar{s}}$ states scatter in a wide range of about 2.4–3.0 GeV. The masses of the low-lying 1P-wave states may highly overlap with the heaviest 1S-wave state $T_{(ss\bar{s}\bar{s})0^{++}}(2440)$.

1. 0^{-+} states

There are three 0^{-+} states, $T_{(ss\bar{s}\bar{s})0^{-+}}(2481)$, $T_{(ss\bar{s}\bar{s})0^{-+}}(2635)$, and $T_{(ss\bar{s}\bar{s})0^{-+}}(2761)$, predicted in the NRPQM. They are mixed states with two color structures $|6\bar{6}\rangle_c$ and $|\bar{3}3\rangle_c$ and also mixed states between two orbital excitations (ξ_1, ξ_2) and ξ_3 modes. They can decay into $\phi h_1(1P)$ via an S wave, or $\phi\phi$ via a P wave, through the quark rearrangements.

In 2016, the BESIII Collaboration observed a new resonance $X(2500)$ with a mass of $2470^{+15+101}_{-19-23}$ MeV and a width of 230^{+64+56}_{-35-33} MeV in $J/\psi \to \gamma\phi\phi$ [12]. The preferred spin-parity numbers for $X(2500)$ are $J^{PC} = 0^{-+}$ [12]. The $X(2500)$ resonance may be a candidate for $T_{(ss\bar{s}\bar{s})0^{-+}}(2481)$ in terms of mass, decay modes, and quantum numbers although $X(2500)$ may favor the 4^1S_0 $s\bar{s}$ state as suggested in our previous work [2]. In the recent work of Ref. [14], the authors also suggested $X(2500)$ to be a 0^{-+} $T_{ss\bar{s}\bar{s}}$ state according to the QCD sum rule studies. A measurement of the branching fraction of $\mathcal{B}[X(2500) \to \phi\phi]$ might provide a test of the nature of $X(2500)$. The decay rate of $T_{(ss\bar{s}\bar{s})0^{-+}}(2481)$ into $\phi\phi$ through the quark rearrangements should be significantly larger than that via an $s\bar{s}$ pair production for the 4^1S_0 $s\bar{s}$ state.

2. 1^{--} states

There are five 1^{--} states, $T_{(ss\bar{s}\bar{s})1^{--}}(2445)$, $T_{(ss\bar{s}\bar{s})1^{--}}(2567)$, $T_{(ss\bar{s}\bar{s})1^{--}}(2627)$, $T_{(ss\bar{s}\bar{s})1^{--}}(2766)$, and $T_{(ss\bar{s}\bar{s})1^{--}}(2984)$, predicted in the NRPQM. Their masses scatter in a rather wide range of about 2.4–3.0 GeV. From Table III, it is found that there are obvious configuration mixings in these tetraquark states except that $T_{(ss\bar{s}\bar{s})1^{--}}(2627)$ may nearly be a pure $^1P_{1^{--}(\bar{3}3)_c(\xi_3)}$ state. The lowest state $T_{(ss\bar{s}\bar{s})1^{--}}(2445)$ is dominated by the $^3P_{1^{--}(6\bar{6})_c(\xi_1,\xi_2)}$ configuration. Its orbital excitation mainly occurs within the diquark (ss) or antidiquark $(\bar{s}\bar{s})$. Meanwhile, the highest state $T_{(ss\bar{s}\bar{s})1^{--}}(2984)$ is dominated by the $^1P_{1^{--}(6\bar{6})_c(\xi_3)}$ configuration, and the orbital excitation occurs between the diquark (ss) and antidiquark $(\bar{s}\bar{s})$.

The vector meson $\phi(2170)$ in RPP [1] is suggested to be a 1^{--} $T_{ss\bar{s}\bar{s}}$ state in the literature [5–10] since it is hard to be explained as a conventional meson state according to its measured decay modes [51,52]. Furthermore, the $X(2239)$ resonance, which was observed in $e^+e^- \to K^+K^-$ by the BESIII Collaboration [11], was suggested to be a candidate of the lowest 1^{--} $T_{ss\bar{s}\bar{s}}$ state by comparing with the mass spectrum from the relativized quark model [4] and the QCD

two-point sum rule method [53]. However, our calculations indicate that neither $\phi(2170)$ nor $X(2239)$ can be assigned to a 1^{--} $T_{ss\bar{s}\bar{s}}$ state since their measured masses are much lower than our predictions. It should be mentioned that in recent studies $\phi(2170)$ was considered as a vector tetraquark state with content $su\bar{s}\bar{u}$ rather than as a state $ss\bar{s}\bar{s}$ [23,54].

The 1^{--} $T_{ss\bar{s}\bar{s}}$ states may have large decay rates into the $f_0(980)\phi$ via an S wave, or into $\eta\phi$ and $\eta'\phi$ via a P wave. There are some experimental evidences for structures around 2.4 GeV observed in the $f_0(980)\phi$ invariant mass spectrum from *BABAR* [55,56], Belle [57], BESII [58], and BESIII [59], which could be signals of the 1^{--} $ss\bar{s}\bar{s}$ tetraquark states [60]. For the heavier states $T_{(ss\bar{s}\bar{s})1^{--}}(2766)$ and $T_{(ss\bar{s}\bar{s})1^{--}}(2984)$, they can also decay into $\Xi\bar{\Xi}$ baryon pair through a $q\bar{q}$ pair production in vacuum. Thus, experimental search for these states in $e^+e^- \to \Xi\bar{\Xi}$ should be very interesting.

3. 1^{-+} states

There are three 1^{-+} states, $T_{(ss\bar{s}\bar{s})1^{-+}}(2564)$, $T_{(ss\bar{s}\bar{s})1^{-+}}(2632)$, and $T_{(ss\bar{s}\bar{s})1^{-+}}(2778)$, predicted in the NRPQM. Note that 1^{-+} are exotic quantum numbers which cannot be accommodated by the conventional $q\bar{q}$ scenario. Both the lowest mass state $T_{(ss\bar{s}\bar{s})1^{-+}}(2564)$ and highest mass state $T_{(ss\bar{s}\bar{s})1^{-+}}(2778)$ are mixed states between the two color structures $|6\bar{6}\rangle_c$ and $|\bar{3}3\rangle_c$, and their orbital excitations are dominated by the (ξ_1, ξ_2) mode. The middle state $T_{(ss\bar{s}\bar{s})1^{-+}}(2632)$ is dominated by the $^3P_{1^{-+}(\bar{3}3)_c(\xi_3)}$ configuration of which the orbital excitation mainly occurs between the diquark (ss) and antidiquark $(\bar{s}\bar{s})$. It should be noted that a corresponding state in the relativized quark model [4] has a mass of 2581 MeV, which is about 50 MeV smaller than our prediction.

These 1^{-+} $T_{ss\bar{s}\bar{s}}$ states may easily decay into $\phi h_1(1P)$, $\eta^{(')} f_1(1420)$, $\phi\phi$ channels through the quark rearrangements. They can be searched for in $\chi_{cJ}(1P) \to \eta\phi\phi, \phi K^* K$ with sufficient $\chi_{cJ}(1P)$ data samples at BESIII, although no obvious structures were found in previous observations [61,62].

4. 2^{-+} states

There are three 2^{-+} states, $T_{(ss\bar{s}\bar{s})2^{-+}}(2537)$, $T_{(ss\bar{s}\bar{s})2^{-+}}(2669)$, and $T_{(ss\bar{s}\bar{s})2^{-+}}(2837)$, predicted in the NRPQM. Both the lowest mass state $T_{(ss\bar{s}\bar{s})2^{-+}}(2537)$ and highest mass state $T_{(ss\bar{s}\bar{s})2^{-+}}(2837)$ are mixed states between the two color structures $|6\bar{6}\rangle_c$ and $|\bar{3}3\rangle_c$. Their orbital excitations are dominated by the (ξ_1, ξ_2) mode. The middle state $T_{(ss\bar{s}\bar{s})2^{-+}}(2669)$ is dominated by the $^3P_{2^{-+}(\bar{3}3)_c(\xi_3)}$ configuration of which the orbital excitation occurs between the diquark (ss) and antidiquark $(\bar{s}\bar{s})$. A corresponding state in the relativized quark model [4] has a

mass of 2619 MeV, which is about 50 MeV smaller than our prediction.

These 2^{-+} $T_{ss\bar{s}\bar{s}}$ states may easily fall apart into $\phi h_1(1P)$ and $\eta f_2'(1525)$ in an S wave, or into $\phi\phi$ in a P wave through the quark rearrangements. For the high mass state $T_{(ss\bar{s}\bar{s})2^{-+}}(2837)$, the strong decay mode $\Xi\bar{\Xi}$ also opens. These states can be searched for in $\chi_{c2}(1P) \to \eta T_{(ss\bar{s}\bar{s})2^{-+}} \to \eta\eta f_2'(1525) \to \eta\eta K\bar{K}$ at BESIII with the sufficient $\chi_{c2}(1P)$ data samples.

5. 0^{--} states

There are two states with exotic quantum numbers of 0^{--}, $T_{(ss\bar{s}\bar{s})0^{--}}(2507)$ and $T_{(ss\bar{s}\bar{s})0^{--}}(2821)$, predicted in the NRPQM. These two states have a strong mixing between the two color structures $|6\bar{6}\rangle_c$ and $|\bar{3}3\rangle_c$. The orbital excitation is the (ξ_1, ξ_2) mode, i.e., the excitation occurs within the diquark (ss) or antidiquark $(\bar{s}\bar{s})$. These two states may have large decay rates into $\phi f_1(1285)$ and $\phi f_1(1420)$ in an S wave, or into $\eta\phi$ and $\eta'\phi$ in a P wave through the quark rearrangements. These 0^{--} exotic states may be produced by the reactions $e^+e^- \to \eta^{(\prime)}X \to \eta^{(\prime)}\eta^{(\prime)}\phi$ or $J/\psi \to \eta^{(\prime)}\eta^{(\prime)}\phi$.

6. 2^{--} states

There are three 2^{--} states, $T_{(ss\bar{s}\bar{s})2^{--}}(2446)$, $T_{(ss\bar{s}\bar{s})2^{--}}(2657)$, and $T_{(ss\bar{s}\bar{s})2^{--}}(2907)$, predicted in the NRPQM. Both the lowest mass state $T_{(ss\bar{s}\bar{s})2^{--}}(2446)$ and highest mass state $T_{(ss\bar{s}\bar{s})2^{--}}(2907)$ are mixed states between the two color structures, $|6\bar{6}\rangle_c$ and $|\bar{3}3\rangle_c$, and their orbital excitations are dominated by the (ξ_1, ξ_2) mode. The middle state $T_{(ss\bar{s}\bar{s})2^{--}}(2657)$ is dominated by the $^3P_{2^{--}(\bar{3}3)_c(\xi_3)}$ configuration, of which the orbital excitation occurs between the diquark (ss) and antidiquark $(\bar{s}\bar{s})$. A corresponding state in the relativized quark model [4] has a mass of 2622 MeV, which is consistent with our prediction. These 2^{--} states may easily decay into $\phi f_1(1285)$, $\phi f_1(1420)$, and $\phi f_2'(1525)$ in an S wave, or into $\eta\phi$, $\eta'\phi$ in a P wave through the quark rearrangements. They can also be searched for in $e^+e^- \to \eta^{(\prime)}X \to \eta^{(\prime)}\eta^{(\prime)}\phi$ or vector charmonium decays such as $J/\psi \to \eta\eta\phi$.

7. 3^{--} state

There is only one 3^{--} state $T_{(ss\bar{s}\bar{s})3^{--}}(2719)$ predicted in the NRPQM. This state has a pure color structure $|\bar{3}3\rangle_c$ and also a pure orbital excitation between the diquark (ss) and antidiquark $(\bar{s}\bar{s})$. Our predicted mass is about 60 MeV larger than that predicted by the relativized quark model [4] with a diquark approximation. The 3^{--} states may easily decay into $\phi f_2'(1525)$ in an S wave by the quark rearrangements. Since it has a high spin, it may be produced relatively easier in $p\bar{p}$ or pp collisions.

IV. SUMMARY

In this work, we calculate the mass spectra for the $1S$, $1P$, and $2S$-wave $T_{ss\bar{s}\bar{s}}$ states in a nonrelativistic potential quark model without the often-adopted diquark-antidiquark approximation. The $1S$-wave ground states lie in the mass range of ~2.21–2.44 GeV, while the $1P$- and $2S$-wave states scatter in a rather wide mass range of ~2.44–2.99 GeV. For the $2S$-wave states, except for the highest state $T_{(ss\bar{s}\bar{s})0^{++}}(3208)$, all the other states lie in a relatively narrow range of ~2.78–2.98 GeV. We find that most of the physical states are mixed states with different configurations.

For the $ss\bar{s}\bar{s}$ system, it shows that both the kinetic energy $\langle T \rangle$ and the linear confinement potential $\langle V^{\mathrm{Lin}} \rangle$ contribute a large positive value to the mass, while the Coulomb-type potential $\langle V^{\mathrm{Coul}} \rangle$ has a large cancellation with these two terms. The spin-spin interaction $\langle V^{SS} \rangle$, tensor potential $\langle V^T \rangle$, and/or the spin-orbit interaction term $\langle V^{LS} \rangle$ also have sizable contributions to some configurations.

Some $T_{ss\bar{s}\bar{s}}$ states may have shown hints in experiment. For instance, the observed decay modes and masses of $f_0(2200)$ and $f_2(2340)$ listed in RPP [1] could be good candidates for the ground states $T_{(ss\bar{s}\bar{s})0^{++}}(2218)$ and $T_{(ss\bar{s}\bar{s})2^{++}}(2378)$, respectively. The newly observed $X(2500)$ at BESIII may be a candidate for the lowest mass $1P$-wave 0^{-+} state $T_{(ss\bar{s}\bar{s})0^{-+}}(2481)$. Another 0^{++} ground state $T_{(ss\bar{s}\bar{s})0^{++}}(2440)$ may have shown signals in the $\phi\phi$ channel at BESIII [12,48]. Our calculation shows that $\phi(2170)$ may not favor a vector state of $T_{ss\bar{s}\bar{s}}$, because of the much higher mass obtained in our model.

It should be stressed that as a flavor partner of $T_{cc\bar{c}\bar{c}}$, the $T_{ss\bar{s}\bar{s}}$ system may have very different dynamic features that need further studies. One crucial point is that the strange quark is rather light and the light flavor mixing effects could become non-negligible. It suggests that strong couplings between $T_{ss\bar{s}\bar{s}}$ and open strangeness channels could be sizable. As a consequence, mixings between $T_{ss\bar{s}\bar{s}}$ and $T_{sq\bar{s}\bar{q}}$ would be inevitable. For an S-wave strong coupling, it may also lead to configuration mixings which can be interpreted as hadronic molecules for a near-threshold structure. In such a sense, this study can set up a reference on the basis of orthogonal states. More elaborated dynamics can be investigated by including the hadron interactions in the Hamiltonian. For states with exotic quantum numbers, experimental searches for their signals can be carried out at BESIII and Belle-II.

[1] M. Tanabashi *et al.* (Particle Data Group), Review of particle physics, Phys. Rev. D **98,** 030001 (2018).

[2] Q. Li, L. C. Gui, M. S. Liu, Q. F. L, and X. H. Zhong, Strangeonium meson spectrum in a constituent quark model, arXiv:2004.05786.

[3] D. Ebert, R. N. Faustov, and V. O. Galkin, Masses of light tetraquarks and scalar mesons in the relativistic quark model, Eur. Phys. J. C **60,** 273 (2009).

[4] Q. F. Lü, K. L. Wang, and Y. B. Dong, The $ss\bar{s}\bar{s}$ tetraquark states and the newly observed structure $X(2239)$ by BESIII Collaboration, Chin. Phys. C **44,** 024101 (2020).

[5] Z. G. Wang, Analysis of the $Y(2175)$ as a tetraquark state with QCD sum rules, Nucl. Phys. **A791,** 106 (2007).

[6] H. X. Chen, X. Liu, A. Hosaka, and S. L. Zhu, The $Y(2175)$ state in the QCD sum rule, Phys. Rev. D **78,** 034012 (2008).

[7] H. X. Chen, C. P. Shen, and S. L. Zhu, A possible partner state of the $Y(2175)$, Phys. Rev. D **98,** 014011 (2018).

[8] H. W. Ke and X. Q. Li, Study of the strong decays of $\phi(2170)$ and the future charm-tau factory, Phys. Rev. D **99,** 036014 (2019).

[9] Z. G. Wang, Light tetraquark state candidates, Adv. High Energy Phys. **2020,** 6438730 (2020).

[10] C. Deng, J. Ping, F. Wang, and T. Goldman, Tetraquark state and multibody interaction, Phys. Rev. D **82,** 074001 (2010).

[11] M. Ablikim *et al.* (BESIII Collaboration), Measurement of $e^+e^- \rightarrow K^+K^-$ cross section at $\sqrt{s} = 2.00$–3.08 GeV, Phys. Rev. D **99,** 032001 (2019).

[12] M. Ablikim *et al.* (BESIII Collaboration), Observation of pseudoscalar and tensor resonances in $J/\psi \rightarrow \gamma\phi\phi$, Phys. Rev. D **93,** 112011 (2016).

[13] M. Ablikim *et al.* (BESIII Collaboration), Observation and study of the decay $J/\psi \rightarrow \phi\eta\eta'$, Phys. Rev. D **99,** 112008 (2019).

[14] R. R. Dong, N. Su, H. X. Chen, E. L. Cui, and Z. Y. Zhou, QCD sum rule studies on the $ss\bar{s}\bar{s}$ tetraquark states of $J^{PC} = 0^{-+}$, Eur. Phys. J. C **80,** 749 (2020).

[15] E. L. Cui, H. M. Yang, H. X. Chen, W. Chen, and C. P. Shen, QCD sum rule studies of $ss\bar{s}\bar{s}$ tetraquark states with $J^{PC} = 1^{+-}$, Eur. Phys. J. C **79,** 232 (2019).

[16] R. Aaij *et al.* (LHCb Collaboration), Observation of structure in the J/ψ-pair mass spectrum, Sci. Bull. **65,** 1983 (2020).

[17] Q. F. L, D. Y. Chen, and Y. B. Dong, Masses of fully heavy tetraquarks $QQ\bar{Q}\bar{Q}$ in an extended relativized quark model, Eur. Phys. J. C **80,** 871 (2020).

[18] H. X. Chen, W. Chen, X. Liu, and S. L. Zhu, Strong decays of fully-charm tetraquarks into di-charmonia, Sci. Bull. **65,** 1994 (2020).

[19] X. Jin, Y. Xue, H. Huang, and J. Ping, Full-heavy tetraquarks in constituent quark models, Eur. Phys. J. C **80,** 1083 (2020).

[20] Z. G. Wang, Tetraquark candidates in the LHCb's di-J/ψ mass spectrum, Chin. Phys. C **44,** 113106 (2020).

[21] M. S. liu, F. X. Liu, X. H. Zhong, and Q. Zhao, Full-heavy tetraquark states and their evidences in the LHCb di-J/ψ spectrum, arXiv:2006.11952.

[22] Y. R. Liu, H. X. Chen, W. Chen, X. Liu, and S. L. Zhu, Pentaquark and tetraquark states, Prog. Part. Nucl. Phys. **107,** 237 (2019).

[23] S. Agaev, K. Azizi, and H. Sundu, Four-quark exotic mesons, Turk. J. Phys. **44,** 95 (2020).

[24] E. Eichten, K. Gottfried, T. Kinoshita, K. D. Lane, and T. M. Yan, Charmonium: The model, Phys. Rev. D **17,** 3090 (1978); **21,** 313(E) (1980).

[25] W. J. Deng, H. Liu, L. C. Gui, and X. H. Zhong, Charmonium spectrum and their electromagnetic transitions with higher multipole contributions, Phys. Rev. D **95,** 034026 (2017).

[26] W. J. Deng, H. Liu, L. C. Gui, and X. H. Zhong, Spectrum and electromagnetic transitions of bottomonium, Phys. Rev. D **95,** 074002 (2017).

[27] M. S. Liu, Q. F. Lü, and X. H. Zhong, Triply charmed and bottom baryons in a constituent quark model, Phys. Rev. D **101,** 074031 (2020).

[28] M. S. Liu, K. L. Wang, Q. F. L, and X. H. Zhong, Ω baryon spectrum and their decays in a constituent quark model, Phys. Rev. D **101,** 016002 (2020).

[29] M. S. Liu, Q. F. Lü, X. H. Zhong, and Q. Zhao, All-heavy tetraquarks, Phys. Rev. D **100,** 016006 (2019).

[30] S. Godfrey and N. Isgur, Mesons in a relativized quark model with chromodynamics, Phys. Rev. D **32,** 189 (1985).

[31] T. Barnes, S. Godfrey, and E. S. Swanson, Higher charmonia, Phys. Rev. D **72,** 054026 (2005).

[32] S. Godfrey, Spectroscopy of B_c mesons in the relativized quark model, Phys. Rev. D **70,** 054017 (2004).

[33] S. Godfrey and K. Moats, Bottomonium mesons and strategies for their observation, Phys. Rev. D **92,** 054034 (2015).

[34] O. Lakhina and E. S. Swanson, A canonical $D_s(2317)$?, Phys. Lett. B **650,** 159 (2007).

[35] Q. F. Lü, T. T. Pan, Y. Y. Wang, E. Wang, and D. M. Li, Excited bottom and bottom-strange mesons in the quark model, Phys. Rev. D **94,** 074012 (2016).

[36] D. M. Li, P. F. Ji, and B. Ma, The newly observed open-charm states in quark model, Eur. Phys. J. C **71,** 1582 (2011).

[37] J. Vijande, A. Valcarce, and N. Barnea, Exotic meson-meson molecules and compact four-quark states, Phys. Rev. D **79**, 074010 (2009).

[38] E. Hiyama, Y. Kino, and M. Kamimura, Gaussian expansion method for few-body systems, Prog. Part. Nucl. Phys. **51**, 223 (2003).

[39] E. Hiyama and M. Kamimura, Study of various few-body systems using Gaussian expansion method (GEM), Front. Phys. (Beijing) **13**, 132106 (2018).

[40] E. Hiyama, M. Kamimura, A. Hosaka, H. Toki, and M. Yahiro, Five-body calculation of resonance and scattering states of pentaquark system, Phys. Lett. B **633**, 237 (2006).

[41] E. Hiyama, A. Hosaka, M. Oka, and J. M. Richard, Quark model estimate of hidden-charm pentaquark resonances, Phys. Rev. C **98**, 045208 (2018).

[42] Q. Meng, E. Hiyama, K. U. Can, P. Gubler, M. Oka, A. Hosaka, and H. Zong, Compact $sssc\bar{c}$ pentaquark states predicted by a quark model, Phys. Lett. B **798**, 135028 (2019).

[43] Q. Meng, E. Hiyama, A. Hosaka, M. Oka, P. Gubler, K. U. Can, T. T. Takahashi, and H. S. Zong, Stable double-heavy tetraquarks: Spectrum and structure, arXiv:2009.14493.

[44] K. Varga and Y. Suzuki, Stochastic variational method with a correlated Gaussian basis, Phys. Rev. A **53**, 1907 (1996).

[45] K. Varga, Y. Ohbayasi, and Y. Suzuki, Stochastic variational method with noncentral forces, Phys. Lett. B **396**, 1 (1997).

[46] K. Varga and Y. Suzuki, Solution of few body problems with the stochastic variational method: 1. Central forces, Comput. Phys. Commun. **106**, 157 (1997).

[47] D. M. Brink and F. Stancu, Tetraquarks with heavy flavors, Phys. Rev. D **57**, 6778 (1998).

[48] A. A. Kozhevnikov, Dynamical analysis of the X resonance contributions to the decay $J/\psi \to \gamma X \to \gamma \phi \phi$, Phys. Rev. D **99**, 014019 (2019).

[49] R. Aaij *et al.* (LHCb Collaboration), Observation of the $B_s^0 \to J/\psi \phi \phi$ decay, J. High Energy Phys. 03 (2016) 040.

[50] A. A. Kozhevnikov, $\phi \phi$ and $J/\psi \phi$ mass spectra in decay $B_s^0 \to J/\psi \phi \phi$, Phys. Rev. D **95**, 014005 (2017).

[51] M. Ablikim *et al.* (BESIII Collaboration), Observation of a Resonant Structure in $e^+ e^- \to K^+ K^- \pi^0 \pi^0$, Phys. Rev. Lett. **124**, 112001 (2020).

[52] M. Ablikim *et al.* (BESIII Collaboration), Observation of a structure in $e^+ e^- \to \phi \eta'$ at $\sqrt{s}$ from 2.05 to 3.08 GeV, Phys. Rev. D **102**, 012008 (2020).

[53] K. Azizi, S. S. Agaev, and H. Sundu, Light axial-vector and vector resonances $X(2100)$ and $X(2239)$, Nucl. Phys. **B948**, 114789 (2019).

[54] S. S. Agaev, K. Azizi, and H. Sundu, Nature of the vector resonance $Y(2175)$, Phys. Rev. D **101**, 074012 (2020).

[55] B. Aubert *et al.* (BABAR Collaboration), The $e^+ e^- \to K^+ K^- \pi^+ \pi^-$, $K^+ K^- \pi^0 \pi^0$ and $K^+ K^- K^+ K^-$ cross-sections measured with initial-state radiation, Phys. Rev. D **76**, 012008 (2007).

[56] B. Aubert *et al.* (BABAR Collaboration), A structure at 2175-MeV in $e^+ e^- \to \phi f_0(980)$ observed via initial-state radiation, Phys. Rev. D **74**, 091103 (2006).

[57] C. P. Shen *et al.* (Belle Collaboration), Observation of the $\phi(1680)$ and the $Y(2175)$ in $e^+ e^- \to \phi \pi^+ \pi^-$, Phys. Rev. D **80**, 031101 (2009).

[58] M. Ablikim *et al.* (BES Collaboration), Observation of $Y(2175)$ in $J/\psi \to \eta \phi f_0(980)$, Phys. Rev. Lett. **100**, 102003 (2008).

[59] M. Ablikim *et al.* (BESIII Collaboration), Study of $J/\psi \to \eta \phi \pi^+ \pi^-$ at BESIII, Phys. Rev. D **91**, 052017 (2015),

[60] H. X. Chen, C. P. Shen, and S. L. Zhu, A possible partner state of the $Y(2175)$, Phys. Rev. D **98**, 014011 (2018),

[61] M. Ablikim *et al.* (BESIII Collaboration), Observation of the decays $\chi_{cJ} \to \phi \phi \eta$, Phys. Rev. D **101**, 012012 (2020).

[62] M. Ablikim *et al.* (BESIII Collaboration), Study of χ_{cJ} decaying into $\phi K^*(892) \bar{K}$, Phys. Rev. D **91**, 112008 (2015).